Journal of the Saudi Society of Agricultural Sciences (2026) 25:43
https://doi.org/10.1007/s44447-026-00136-w

RESEARCH

# Enhancing the recovery of bioactive compounds from rain tree (*Samanea saman*) seeds through optimized ultrasound-assisted extraction and response surface methodology

**Gad Elsayed Mohamed Salem[1,2] · Mohammad Fikry[3,4] · Kittaporn Ngiwngam[1,2] · Patcharee Pripdeevech[5,6] · Wirongrong Tongdeesoontorn[1,2]**

Received: 18 November 2025 / Accepted: 3 February 2026
© The Author(s) 2026

## Abstract

This study aimed to optimize ultrasound-assisted extraction (UAE) of phytochemicals and antioxidant properties from rain tree seed extract (RTSE) by evaluating ultrasonic power ratio, extraction temperature, extraction time, and ethanol concentration. Increasing power from 20 to 80% decreased total flavonoid content (TFC) and ferric reducing antioxidant power (FRAP) by 25–37%. Higher extraction temperatures (70°C) reduced antioxidant activities by up to 35% compared with mid-range conditions (50–60°C). Prolonged extraction times (50 min) caused declines of up to 28% in TFC and DPPH activity, showing the sensitivity of flavonoids to extended exposure. In contrast, total phenolic content (TPC) increased by 12–20% with higher temperature and time, suggesting thermal facilitation of phenolic release. Ethanol concentration displayed a parabolic effect, with 30–40% producing the best yield, while 10% or 50% caused 15–25% reductions. Second-order polynomial models accurately predicted extraction yield (EY), TPC, TFC, DPPH scavenging activity, and FRAP. The optimal UAE conditions 44% power, 60°C, 10 min, and 23% ethanol produced an EY of 17.36%, TPC of 0.0147 mg GAE/g DW, TFC of 0.033 mg QE/g DW, 60.44% DPPH activity, and 5.97 mmol $Fe^{2+}$/g DW FRAP, closely matching predicted values. LC-QTOF-MS profiling of the optimized extract revealed a metabolome dominated by flavonoid glycosides, phenolic esters, and isoflavones, with oxylipins and glycolipids also present. Major compounds included quercetin and luteolin derivatives, phenolic esters, and plant hormone conjugates. These findings highlight rain tree seeds as a rich source of bioactive compounds with potential applications in functional foods.

**Keywords** Bioactive compounds · Box-behnken design · Energy consumption · Mathematical modelling · Optimization · Rain tree seeds · Ultrasound-assisted extraction

✉ Wirongrong Tongdeesoontorn
wirongrong.ton@mfu.ac.th

Gad Elsayed Mohamed Salem
gadelnagar@yahoo.com

Mohammad Fikry
moh.eltahlawy@fagr.bu.edu.eg

Kittaporn Ngiwngam
6671401004@lamduan.mfu.ac.th

Patcharee Pripdeevech
patcharee.pri@mfu.ac.th

[1] School of Agro-Industry, Mae Fah Luang University, 333 Moo 1 Tasud, Chiang Rai 57100, Thailand

[2] Research Center of Innovative Food Packaging and Biomaterials Unit, Mae Fah Luang University, 333 Moo 1 Tasud, Chiang Rai 57100, Thailand

[3] Date Palm Research Center of Excellence, King Faisal University, Al Hufuf 31982, Saudi Arabia

[4] Department of Agricultural and Biosystems Engineering, Faculty of Agriculture, Benha University, Moshtohor, 13736 Toukh, Egypt

[5] School of Science, Mae Fah Luang University, Chiang Rai 57100, Thailand

[6] Center of Chemical Innovation for Sustainability (CIS), Mae Fah Luang University, Chiang Rai 57100, Thailand

Published online: 12 March 2026

## 1 Introduction

The rain tree (*Samanea saman*) belongs to the Fabaceae family. It is commonly called the "rain tree" because its leaves are sensitive to light, allowing raindrops to pass through and reach the ground below. Native to northern South America, from Mexico to Colombia, the rain tree is now widely distributed throughout tropical regions. (Boppena et al. 2023). Rain tree fruits (pods) are 8–20 cm long and turn from green to dark brown when mature. Each pod contains 5–10 seeds embedded in a sweet, energy-rich pulp. Owing to their high digestibility and substantial protein (16–30%) and sugar (18–30%) contents, rain tree pods are a valuable energy and protein source for animal feed in tropical regions (Delgado et al. 2014).

The seeds of rain trees are increasingly recognized for their ecological, nutritional, and medicinal benefits. These seeds are rich in bioactive compounds, like phenolics, which can act as antioxidants, anti-inflammatories, and antimicrobials. Extracted oil can be used to produce biolubricants, biodiesel, bio-pesticides, bio-fertilizers, and paints, as well as shampoos, soaps, and detergents (Boppena et al. 2023). To maximize the value of these seeds, all components, especially phenolic compounds, must be extracted comprehensively. The combination of high phenolic compound content and high antioxidant capacity makes plant extracts a potential treatment for diseases associated with oxidative stress, such as diabetes and cancer (Shi et al. 2022).

Conventional extraction methods, such as maceration and Soxhlet extraction, are commonly used to obtain extracts from food materials. These techniques typically rely on significant volumes of organic solvents and require extended processing times and elevated temperatures, which can compromise the integrity of sensitive bioactive compounds (Dorta et al. 2013). Additionally, the use of organic solvents poses safety and environmental concerns due to their potential toxicity and ecological impact.

In response to these limitations, there has been a growing emphasis on developing environmentally friendly or “green” extraction technologies. These innovative approaches aim to reduce solvent usage, minimize energy consumption, and preserve the functional properties of bioactive compounds (Tiwari 2015).. Many of these methods are designed to operate under milder conditions, thereby enhancing extract quality and safety. As such, green extraction techniques represent a promising alternative for maximizing the recovery of phytochemicals from plant sources while addressing health, safety, and sustainability concerns (Mason et al. 2011; Chemat et al. 2012).

Ultrasound-assisted extraction (UAE) is a sustainable and innovative technique that utilizes high-frequency sound waves (above 20 kHz) to enhance the extraction of bioactive compounds from food matrices (Awad et al. 2012). This method is recognized for its efficiency, reduced processing time, lower solvent and energy consumption, and its ability to preserve the nutritional and functional qualities of the extract (Oyedeji et al. 2016; Fikry et al. 2021, 2023).

When applied to materials immersed in liquid or osmotic media, ultrasound promotes mechanical vibrations that induce alternating compression and expansion cycles. These actions generate microscopic channels within the food matrix, significantly improving mass transfer (Oladejo et al. 2017). Additionally, the ultrasonic waves create cavitation—tiny bubbles that collapse violently leading to cell disruption and structural alterations through localized shockwaves (Wiktor et al. 2019).

UAE has proven effective for extracting phytochemicals from a wide range of plant-based sources, including black jamun pulp (Sharma and Dash 2022), *Inula viscosa* (Aydar et al. 2022), Ruby S apple peel (Park et al. 2022), mango kernels (Hayat et al. 2023), dragon fruit (Raj and Dash 2020), longan seeds (Fikry et al. 2024a) and *Terminalia chebula* pulp (Jha and Sit 2023). This highlights its versatility and potential as a green technology for bioactive compound recovery across various food processing applications.

To improve the effectiveness of UAE, it is essential to optimize processing conditions and examine the associated thermodynamic parameters. Several studies have utilized predictive models such as general regression models to assess how extraction variables influence the recovery of bioactive compounds (Park et al. 2022; Sai-Ut et al. 2023,). Evaluating thermodynamic parameters provides valuable information on the feasibility and spontaneity of the extraction process. Moreover, studying both the kinetics and thermodynamics of UAE offers deeper understanding of the process mechanisms and supports its practical application in industrial-scale operations (Sharma and Dash 2022).

Prior research has investigated the extraction of bioactive compounds from rain tree seeds utilizing organic solvents through both conventional and UAE methods (Fidan et al. 2020; Ayache et al. 2021). However, to the best of the authors' knowledge, no study has specifically addressed the optimal extraction conditions according to the extraction yield, and phytochemicals properties of UAE for rain tree seed extract (RTSE). Hence, this study aimed to investigate the effects of ultrasonic power ratio, temperature, exposure time and solvent ratio on the extraction yield, total phenolic contents, total flavonoid contents, DPPH radical scavenging activity and FRAP activity during the extraction process using UAE. Furthermore, the research aimed to determine the optimal UAE extraction conditions for RTSE.

## 2 Materials and methods

### 2.1 Chemicals and reagents

Analytical-grade reagents and solvents were used throughout the experiment. Key materials included ethanol from EMSURE® (Germany), methanol from Fisher Scientific (UK), and Folin–Ciocalteu reagent from Carlo Erba (France), 2,2-diphenyl-1-picrylhydrazyl (DPPH) from Fluka (USA). Gallic acid was supplied by Fluka (Spain), aluminum chloride by Ajax Finechem (New Zealand), quercetin by Sigma-Aldrich (Germany), and sodium carbonate by Guangzhou Reagent (China).

### 2.2 Preparation of rain tree seeds powder

Rain tree pods were collected from Mae Fah Luang university campus, Chiang Rai province, Thailand. The seeds were separated manually from pods then cleaned manually to remove any foreign or unwanted material and damaged seeds. The seeds were initially soaked in hot water for one hour to help the removal of any residual pulp. Subsequently this, they were dried in a laboratory oven (BINDER, UN, Schwabach, Germany) at a temperature of $60 \pm 2$ °C and a relative humidity of $50 \pm 1$% for 24 h, until their moisture content reached approximately $0.03 \pm 0.005$ gw/gdm on a dry basis. Once dried, the seeds were allowed to cool to room temperature and then ground into a fine powder using a hammer mill (Perten, 120, Finland) fitted with an 80 µm mesh screen. The resulting powder was stored in airtight polyethylene bags and kept in a refrigerator at $7 \pm 2$ °C to minimize moisture uptake and suppress enzymatic activity.

### 2.3 Preparation of Rain Tree Seeds Extract (RTSE)

To prepare the extracts for determining total phenolic content (TPC), total flavonoid content (TFC), DPPH radical scavenging activity, and Ferric Reducing Antioxidant Power (FRAP), 3 g of rain tree seed powder was mixed with 30 mL of ethanol–water mixtures at various ethanol concentrations (10–50% v/v), maintaining a constant solvent-to-solid ratio of 10 mL/g. This process was adapted with slight modifications from the methods described by Alara and Abdurahman (2019). Extraction was conducted using an ultrasonic homogenizer (SONICS, Model: VCX500, S/N: 106037AS-12–18, SONICS &MATERIALS, INC, U.S.A) with a maximum output of 1200 W. Prior to extraction, the device was adjusted to different ultrasonic power levels 20% (240 W) to 80% (960 W) and set to operate at controlled temperatures (30 °C to 70 °C). The extraction was performed for durations of 10 to 50 min. Following extraction, each sample was centrifuged at 3500 rpm for 10 min using a centrifuge (Model 5310, KUBOTA CORPORATION, Japan), as described by Sharma and Dash (2022). The supernatant was then separated and passed through Whatman No. 1 filter paper to remove solids. To determine the extraction yield, the supernatant mass was measured using a balance and expressed as the ratio of the extract mass to the dry matter mass (Dhanani et al. 2017). The final extracts were stored at − 20 °C until they were analyzed.

### 2.4 Measurements of Total Phenolic Content (TPC)

The Total Phenolic Content (TPC) of the rain tree seed extract (RTSE) samples was determined using a modified version of the procedure described by Wen et al. (2012) and Khalaf 2019). Briefly, 0.1 mL of each RTSE sample was mixed with 5 mL of distilled water, followed by the addition of 0.5 mL of Folin–Ciocalteu reagent. After an 8-min reaction period, 1.5 mL of 20% sodium carbonate ($Na_2CO_3$) was added, and the mixture was left to stand at room temperature for 20 min. Absorbance was then recorded at 765 nm using a UV–vis spectrophotometer (Eppendorf BioSpectrometer® basic, Thailand), with distilled water as the blank. Gallic acid was used as the calibration standard, with a standard curve defined by the equation $y = 0.665x + 0.0904$ ($R^2 = 0.999$), in accordance with Corrales et al. (2008). TPC was expressed as milligrams of gallic acid equivalents per gram of dry weight (mg GAE/g DW). All analyses were performed in triplicate, and results are reported as mean ± standard deviation.

### 2.5 Measurement of Total Flavonoid Content (TFC)

Total flavonoid content (TFC) in rain tree seed extract (RTSE) was determined using a modified method from Silva et al. (2015). A 1 mL aliquot of RTSE was mixed with 1 mL of 2% (w/v) aluminum chloride in methanol and incubated for 30 min at room temperature. Absorbance was recorded at 430 nm using a UV–vis spectrophotometer (Eppendorf BioSpectrometer® basic, Thailand), with distilled water as the blank. TFC was calculated using a quercetin calibration curve ($y = 0.551x + 0.304$, $R^2 = 0.995$) and expressed as mg quercetin equivalents per gram of dry weight (mg QE/g DW). All measurements were conducted in triplicate, and results are reported as mean ± standard deviation.

### 2.6 Determination of DPPH scavenging activity (%)

The antioxidant activity of rain tree seed extract (RTSE) was evaluated using the DPPH radical scavenging assay, adapted from Papoutsis et al. (2017). A DPPH stock solution (24 mg in 100 mL methanol) was prepared and stored at − 22 °C. Prior to analysis, a working solution was made by

diluting 10 mL of stock with 45 mL of methanol to achieve an absorbance of 1.1 ± 0.02 at 517 nm. For the assay, 0.2 mL of RTSE was mixed with 2 mL methanol and 2 mL of the DPPH working solution. The mixture was incubated in the dark at room temperature for 30 min. Absorbance was then measured at 517 nm using a UV–vis spectrophotometer (Eppendorf BioSpectrometer® basic, Thailand), with methanol serving as the blank. Antioxidant capacity was calculated using the corresponding equation (Eq. 1).

$$\% \text{ DPPH antioxident capacity} = \left[1 - \frac{A_{sample}}{A_{control}}\right] x100 \quad (1)$$

where $A_{control}$ refers to the absorbance of the DPPH solution mixed with methanol (without extract), and $A_{sample}$ represents the absorbance of the DPPH solution combined with the extract.

### 2.7 Determination of FRAP activity (%)

The antioxidant capacity of the digested samples was evaluated using the FRAP (Ferric Reducing Antioxidant Power) assay, based on the procedure described by Ketnawa and Ogawa (2019). The FRAP reagent was freshly prepared by mixing a 10 mM TPTZ solution in 40 mM HCl, a 20 mM $FeCl_3 \cdot 6H_2O$ solution, and a 300 mM acetate buffer (pH 3.6) in a 1:1:10 volume ratio. A 0.260 mL aliquot of this reagent was pre-incubated at 37 °C, after which 0.040 mL of the sample was added. The mixture was incubated in the dark at 37 °C for 30 min. Following incubation, the absorbance was read at 590 nm. A blank sample was prepared by replacing the test sample with distilled water. The FRAP results were calculated using a standard curve of $FeSO_4$ (0–100 µmol/L) and reported as micromoles of $FeSO_4$ equivalents per gram of dry sample.

### 2.8 Liquid Chromatography–Quadrupole Time of Flight Mass Spectrometry (LC–QTOF)

The LC-QTOF-MS analysis was conducted on the rain tree seed extract obtained under the optimized UAE conditions determined in this study (44% power ratio, 60 °C, 10 min extraction time, 23% ethanol concentration). The chromatographic analysis was carried out using an Agilent 1290 Infinity LC system equipped with a binary pump, a micro-vacuum degasser, an autosampler (100-well), and a temperature-controlled column compartment. Separation was performed on an Agilent Poroshell 120 EC-C18 column (2.1 × 150 mm, 2.7 µm) operated at 40 °C with a flow rate of 0.2 mL/min. The mobile phase consisted of solvent A (water with 0.1% formic acid) and solvent B (acetonitrile with 0.1% formic acid). The gradient program started at 99% A/1% B and was held for 3 min, followed by a linear increase to 45% B over 27 min, then to 100% B in the next 10 min. After each run, the column was washed with 100% B for 5 min and re-equilibrated with the initial composition (99% A/1% B) for 5 min. The injection volume was 1 µL.

Mass spectrometric detection was carried out on an Agilent 6200/6500 series Q-TOF mass spectrometer (Agilent Technologies, Santa Clara, CA, USA) fitted with an electrospray ionization (ESI) source. The operating conditions were as follows: drying gas ($N_2$) at 13 L/min and 325 °C, sheath gas at 11 L/min and 325 °C, nebulizer pressure 27 psig, capillary voltage 3500 V, skimmer 65 V, octopole RF voltage 750 V, and fragmentor voltage 150 V. The collision energy was set to 45 eV. Data acquisition and control were performed with Agilent MassHunter Acquisition Software (version A.10.00), and data processing was conducted using MassHunter Qualitative Analysis Software (version B.10.0). Spectra were acquired in both positive and negative ionization modes across the m/z range 50–1700. For internal mass calibration, reference ions at m/z 121.0509 (protonated purine) and 922.0098 [protonated hexakis(1H,1H,3H-tetrafluoropropoxy) phosphazine, HP-921] were used in positive mode, while m/z 112.9856 (deprotonated trifluoroacetic acid, TFA) and 1033.9881 (TFA-adducted HP-921) were used in negative mode. All detected compounds were verified based on accurate mass and reference ion correction (Avula et al. 2023).

### 2.9 Experimental design and data analysis

A structured Box-Behnken Design (BBD) with four factors, Power Ratio (20–80%), Temperature (30–70°C), Time (10–50 min), and Solvent Ratio (10–50%) were employed to systematically evaluate their effects on the response variables. Using preliminary tests, the selected temperature range (30–70°C), time range (10–50 min), ethanol concentration range (10–50%), and ultrasonic amplitude range (20–80%) corresponded to UAE parameters established for extracting thermolabile phenolics from seed matrixes, as demonstrated in a comparable optimization study of longan seeds (Fikry et al. 2024a). The design comprised 27 experimental runs, including (1) 12 edge midpoint combinations to assess two-factor interactions, (2) 8 axial points to explore quadratic effects, and (3) 7 center point replicates (including 5 at the exact midpoint: 50% Power, 50 °C, 30 min, 30% Solvent) to estimate experimental error and curvature. Coded values (− 1, 0, + 1) were assigned to low, center, and high levels of each factor, respectively, to facilitate statistical analysis. This design optimized the number of experiments while ensuring robust estimation of linear, interaction, and quadratic terms for response surface modeling (RSM). Run order was randomized to minimize bias from uncontrolled variables (Table 1). The dependent

**Table 1** Box–Behnken experimental design for optimizing extraction parameters to maximize yield, total phenolic content (TPC), total flavonoid content (TFC), DPPH radical scavenging activity and FRAP activity of rain tree seeds extract

| Run | Independent parameters | | | | Responses | | | | |
|---|---|---|---|---|---|---|---|---|---|
| | $X_1$ | $X_2$ | $X_3$ | $X_4$ | $Y_1$ | $Y_2$ | $Y_3$ | $Y_4$ | $Y_5$ |
| 1 | −1 [20] | −1 [30] | 0 [30] | 0 [30] | 18.10 ± 1.20 | 0.015 ± 0.001 | 0.025 ± 0.0028 | 46.28 ± 1.60 | 6.05 ± 0.60 |
| 2 | 1 [80] | −1 [30] | 0 [30] | 0 [30] | 17.20 ± 0.90 | 0.013 ± 0.019 | 0.020 ± 0.0003 | 55.06 ± 0.17 | 4.99 ± 0.12 |
| 3 | −1 [20] | 1 [70] | 0 [30] | 0 [30] | 18.50 ± 1.10 | 0.014 ± 0.036 | 0.021 ± 0.0007 | 46.40 ± 1.37 | 5.08 ± 0.05 |
| 4 | 1 [80] | 1 [70] | 0 [30] | 0 [30] | 10.30 ± 0.80 | 0.009 ± 0.024 | 0.013 ± 0.0013 | 43.09 ± 3.12 | 5.21 ± 1.40 |
| 5 | −1 [20] | 0 [50] | −1 [10] | 0 [30] | 19.40 ± 1.30 | 0.017 ± 0.076 | 0.024 ± 0.0010 | 43.81 ± 1.82 | 5.65 ± 0.11 |
| 6 | 1 [80] | 0 [50] | −1 [10] | 0 [30] | 17.50 ± 1.00 | 0.016 ± 0.037 | 0.034 ± 0.0052 | 52.36 ± 2.31 | 5.41 ± 0.08 |
| 7 | −1 [20] | 0 [50] | 1 [50] | 0 [30] | 16.20 ± 0.95 | 0.014 ± 0.043 | 0.018 ± 0.0019 | 49.47 ± 3.21 | 5.95 ± 0.18 |
| 8 | 1 [80] | 0 [50] | 1 [50] | 0 [30] | 9.80 ± 0.70 | 0.008 ± 0.065 | 0.015 ± 0.0016 | 49.13 ± 5.02 | 6.05 ± 0.45 |
| 9 | 0 [50] | −1 [30] | −1 [10] | 0 [30] | 19.10 ± 1.25 | 0.015 ± 0.019 | 0.036 ± 0.0097 | 51.64 ± 2.63 | 5.13 ± 0.11 |
| 10 | 0 [50] | 1 [70] | −1 [10] | 0 [30] | 20.20 ± 1.40 | 0.014 ± 0.096 | 0.049 ± 0.0064 | 52.59 ± 2.31 | 5.33 ± 0.14 |
| 11 | 0 [50] | −1 [30] | 1 [50] | 0 [30] | 14.50 ± 0.85 | 0.012 ± 0.011 | 0.038 ± 0.0018 | 62.97 ± 2.80 | 5.61 ± 0.34 |
| 12 | 0 [50] | 1 [70] | 1 [50] | 0 [30] | 10.20 ± 0.75 | 0.008 ± 0.050 | 0.013 ± 0.0026 | 53.58 ± 1.19 | 6.36 ± 0.36 |
| 13 | −1 [20] | 0 [50] | 0 [30] | −1 [10] | 15.50 ± 0.95 | 0.013 ± 0.109 | 0.020 ± 0.0031 | 52.74 ± 0.07 | 5.65 ± 0.09 |
| 14 | 1 [80] | 0 [50] | 0 [30] | −1 [10] | 11.20 ± 0.80 | 0.013 ± 0.133 | 0.007 ± 0.0012 | 49.85 ± 2.37 | 5.83 ± 0.07 |
| 15 | −1 [20] | 0 [50] | 0 [30] | 1 [50] | 20.40 ± 1.45 | 0.016 ± 0.015 | 0.032 ± 0.0062 | 51.15 ± 2.89 | 3.72 ± 0.13 |
| 16 | 1 [80] | 0 [50] | 0 [30] | 1 [50] | 16.20 ± 1.10 | 0.012 ± 0.034 | 0.022 ± 0.0036 | 54.19 ± 1.98 | 4.35 ± 0.14 |
| 17 | 0 [50] | −1 [30] | 0 [30] | −1 [10] | 15.10 ± 0.90 | 0.015 ± 0.044 | 0.017 ± 0.0022 | 52.25 ± 2.05 | 5.23 ± 0.06 |
| 18 | 0 [50] | 1 [70] | 0 [30] | −1 [10] | 13.30 ± 0.85 | 0.014 ± 0.061 | 0.009 ± 0.0035 | 50.08 ± 2.68 | 5.30 ± 0.14 |
| 19 | 0 [50] | −1 [30] | 0 [30] | 1 [50] | 20.20 ± 1.35 | 0.014 ± 0.044 | 0.022 ± 0.0019 | 50.92 ± 0.51 | 3.71 ± 0.09 |
| 20 | 0 [50] | 1 [70] | 0 [30] | 1 [50] | 20.50 ± 1.50 | 0.016 ± 0.007 | 0.015 ± 0.0018 | 49.55 ± 1.33 | 4.19 ± 0.12 |
| 21 | 0 [50] | 0 [50] | −1 [10] | −1 [10] | 12.30 ± 0.75 | 0.017 ± 0.971 | 0.020 ± 0.0024 | 53.20 ± 2.92 | 6.20 ± 1.35 |
| 22 | 0 [50] | 0 [50] | 1 [50] | −1 [10] | 10.40 ± 0.70 | 0.009 ± 0.081 | 0.008 ± 0.0047 | 49.02 ± 6.52 | 5.86 ± 1.34 |
| 23 | 0 [50] | 0 [50] | −1 [10] | 1 [50] | 23.30 ± 1.60 | 0.020 ± 0.016 | 0.016 ± 0.0019 | 27.13 ± 5.59 | 4.67 ± 0.14 |
| 24 | 0 [50] | 0 [50] | 1 [50] | 1 [50] | 18.20 ± 1.25 | 0.014 ± 0.025 | 0.017 ± 0.0035 | 55.78 ± 8.20 | 4.13 ± 0.30 |
| 25 | 0 [50] | 0 [50] | 0 [30] | 0 [30] | 14.50 ± 0.90 | 0.015 ± 0.089 | 0.037 ± 0.0020 | 63.16 ± 3.14 | 6.00 ± 0.28 |
| 26 | 1 [80] | 0 [50] | 0 [30] | 0 [30] | 10.20 ± 0.75 | 0.009 ± 0.091 | 0.018 ± 0.0009 | 38.03 ± 2.29 | 5.07 ± 0.81 |
| 27 | −1 [20] | 1 [70] | 0 [30] | 0 [30] | 18.50 ± 1.20 | 0.017 ± 0.044 | 0.046 ± 0.0002 | 45.37 ± 6.60 | 5.54 ± 0.24 |

Values in the table are presented as the mean ± standard deviation (SD) based on three replicates ($n = 3$).

$X_1$ refers to the power ratio (%), $X_2$ represents the extraction temperature (°C); $X_3$ denotes the extraction time (minutes); $X_4$ refers to ethanol concentration (%). $Y_1$ represents extraction yield (%), $Y_2$ indicates total phenolic content (mg GAE/g DW); $Y_3$ is total flavonoid content (mg QE/g DW); $Y_4$ corresponds to DPPH radical scavenging activity (% inhibition); $Y_5$ denotes FRAP activity (mmol $Fe^{2+}$/g DW).

responses encompassed EC, EY, DPPH, FRAP, TPC, and TFC of the RTSE. Utilizing the polynomial model (Eq. 2) as proposed by Chakraborty et al. (2020), the responses under various conditions have been predicted. Non-linear regression analysis and analysis of variance were employed to assess the effects of the independent variables on the dependent variables. Significance was determined based on p-values, where values below 0.05 were considered significant. Additionally, $R^2$ value of at least 0.90 was used as a criterion to adequately describe the variability of the regression model and the variance of the different properties (Park et al. 2022; Sai-Ut et al. 2023). For experimental design and data analysis, Minitab18 was utilized.

$$y_n = a_0 + \sum_{i=1}^{k} a_i x_i + \sum_{i=1}^{k} a_{ii} x_i x_i + \sum_{i=1}^{k-1} \sum_{j=i+1}^{k} a_{ij} x_i x_j \quad (2)$$

where $y_n$, is the predicted response, while $x_i$ and $x_j$ are the input predictors. $a_0$, $a_i$, $a_{ii}$ and $a_{ij}$ are the intercept, linear, quadratic coefficients and cross-product term of the model, respectively. The terms k denotes the number of input predictors (k = 4 variables).

## 3 Results and discussion

### 3.1 Effect of UAE factors on extraction yield

The extraction yield, defined as the ratio of extract mass to dry matter mass, was employed as an indicator to assess the influence of extraction conditions. EY of RTSE varied between 9.80% and 23.30%. The highest yield was observed in Run 23, which was conducted at power ratio of 50%, 50 °C, 10 min and ethanol concentration of 50 mL/g. These conditions likely provided an optimal balance between solute solubility and diffusion without compromising thermolabile compounds. In contrast, the lowest yield was obtained in Run 8 (80%, 50 °C, 50 min, 50 mL/g ethanol), where the elevated temperature and high ethanol concentration may have led to the degradation or reduced solubility of some extractable solids. This highlights the importance of using moderate temperature and low ethanol concentration combined with a high solvent volume to enhance the extraction efficiency.

As evidenced in Table 2, extraction yield (EY) shows clear dependence on ultrasonication conditions—particularly power ratio, temperature, and duration. The primary role of ultrasonic power lies in ensuring effective solvent permeation through the sample matrix (Han et al. 2011). EY exhibited a strong dependence on ultrasonication power ratio, with systematic variations observed across tested power levels (Table 1). At the low power ratio level (20%), the average yield was generally higher compared to the high level (80%). For instance, run 1 had an EY of 18.10 ± 1.20%, while run 2 recorded a slightly lower EY of 17.20 ± 0.90%. More pronounced differences were observed in other runs: run 7 yielded 16.20 ± 0.95%, whereas run 8 showed a significantly lower yield of 9.80 ± 0.70%, a decrease of nearly 40%. Similarly, runs 15 (20.40 ± 1.45%) and 16 (16.20 ± 1.10%) confirm the trend of higher yields at lower power. This suggests that increasing the power ratio negatively affects extraction yield, possibly due to degradation or unfavorable extraction kinetics at higher energy inputs. Comparable findings were reported by (Dalmau et al. 2020) for orange byproduct extracts across varying acoustic power densities.

Concerning temperature effects during ultrasonication, extraction temperature showed a marked effect on yield, with lower temperatures (30°C) consistently resulting in higher yields than higher temperatures (70°C). For example, runs at 30 °C like run 1 (18.10 ± 1.20%) and run 9 (19.10 ± 1.25%) had higher yields than their counterparts at 70 °C such as run 3 (18.50 ± 1.10%) and run 10 (20.20 ± 1.40%), though in some cases higher temperatures also showed increased yields, indicating a complex interaction with other variables. However, a stark contrast is seen between run 4 (10.30 ± 0.80% at 70 °C) and run 3 (18.50 ± 1.10%

**Table 2** ANOVA results for the proposed model applied in this study

| Terms | EY | | TPC | | TFC | | DPPH | | FRAP | |
|---|---|---|---|---|---|---|---|---|---|---|
| | F-Value | P-value | F-Value | P-value | F-Value | P-value | F-Value | P-value | F-Value | P-value |
| **Regression (Full model)** | 17.24 | 0.019* | 25.2 | 0.011* | 8.32 | 0.054 | 6.03 | 0.083 | 2.86 | 0.21 |
| **Linear** | | | | | | | | | | |
| $x_1$ | 1.07 | 0.377 | 2.24 | 0.231 | 9.58 | 0.053 | 31.99 | 0.011* | 5.72 | 0.097 |
| $x_2$ | 0.28 | 0.635 | 2.97 | 0.183 | 3.45 | 0.16 | 11.52 | 0.043* | 5.58 | 0.099 |
| $x_3$ | 0.45 | 0.549 | 4.5 | 0.124 | 4.45 | 0.125 | 14.48 | 0.032* | 8.82 | 0.059 |
| $x_4$ | 5.21 | 0.107 | 2.42 | 0.218 | 0.25 | 0.654 | 1.56 | 0.301 | 3.68 | 0.151 |
| **Quadratic** | | | | | | | | | | |
| $x_1^2$ | 0 | 0.985 | 0.25 | 0.654 | 10.49 | 0.048* | 23.15 | 0.017* | 3.97 | 0.14 |
| $x_2^2$ | 0.07 | 0.811 | 1.64 | 0.29 | 1.73 | 0.28 | 8.31 | 0.063 | 4.31 | 0.13 |
| $x_3^2$ | 0 | 0.962 | 1.42 | 0.319 | 0.37 | 0.586 | 5.78 | 0.096 | 10.45 | 0.048* |
| **Interaction** | | | | | | | | | | |
| $x_1x_2$ | 12.68 | 0.038* | 6.72 | 0.081 | 0.11 | 0.767 | 7.5 | 0.071 | 2.2 | 0.235 |
| $x_1x_3$ | 4.82 | 0.116 | 17.13 | 0.026* | 2.78 | 0.194 | 4.06 | 0.137 | 0.18 | 0.7 |
| $x_1x_4$ | 0 | 0.977 | 0.08 | 0.794 | 2.63 | 0.203 | 3.27 | 0.168 | 0.5 | 0.532 |
| $x_2x_3$ | 6.94 | 0.078 | 8.8 | 0.059 | 18.37 | 0.023* | 5.49 | 0.101 | 0.46 | 0.545 |
| **$R^2$** | 0.920 | | 0.810 | | 0.720 | | 0.670 | | 0.820 | |
| **Adjusted $R^2$** | 0.860 | | 0.690 | | 0.610 | | 0.580 | | 0.700 | |
| **Predicted $R^2$** | 0.700 | | 0.420 | | 0.380 | | 0.330 | | 0.470 | |
| **Lack of Fit** | ns | | ns | | ns | | ns | | ns | |

*Significant at significance level of 0.05

at 30 °C), where yield decreased by 44.32%. Thus, while moderate temperatures may help increase yield, excessively high temperatures tend to reduce soluble solids extraction, potentially due to thermal degradation or reduced solubility. Our observations correlate with previously reported data for Ruby S apple peel extracts (Park et al. 2022), suggesting consistent behavior across plant matrices.

Like power and temperature effects, extraction duration exhibited a positive but non-linear relationship with EY (Table 1). At shorter extraction times (10 min), yields ranged from 14.50 ± 0.85% (run 11) to 23.30 ± 1.60% (run 23), with the highest yield observed in run 23 at 23.30%. In comparison, longer extraction times (50 min) such as in run 7 (16.20 ± 0.95%) and run 24 (18.20 ± 1.25%) exhibited moderate yields. Although some runs with longer extraction times produced higher yields (e.g., run 20: 20.50 ± 1.50%), the overall trend suggests that increasing extraction time does not uniformly increase yield, and optimal extraction time depends on the interaction with other factors like power ratio and temperature. The maximum yield at 10 min (23.30%) compared to the minimum at 50 min (10.40% in run 22) indicates a possible 55% decrease when extending time under certain conditions. These results confirm the universal time-dependence of ultrasound-assisted extraction first documented (Dalmau et al. 2020).

Ethanol concentration had a variable but notable effect on yield. Lower ethanol concentrations (10%) often resulted in lower yields compared to intermediate concentrations. For example, run 13 had a yield of 15.50 ± 0.95%, whereas run 15 (50%) showed a higher yield of 20.40 ± 1.45%, representing a 31.61% increase. Nonetheless, the effect is not consistent across all runs, as seen in run 23 with a high yield (23.30 ± 1.60%) at and run 26 with a low yield (10.20 ± 0.75%). This suggests ethanol concentration influences extraction yield by modifying solvent polarity, affecting solubility of rain tree seed components, but optimal concentration depends on the interplay with other extraction conditions. These effects may result from the combined action of extraction parameters on rain tree seed morphology—both through tissue softening that improves compound diffusivity and cleavage of recalcitrant polymer networks.

From Table (2), the second-order polynomial model for EY demonstrated an excellent fit, with an $R^2$ value of 0.984, indicating that 98.4% of the variability in EY was explained by the model. The linear coefficients were all positive, suggesting that increasing ultrasonication power, temperature, time, or solvent ratio initially enhanced extraction efficiency. However, the negative quadratic terms revealed a diminishing return at higher parameter levels, implying an optimal threshold beyond which further increases reduce yield. Notably, the interaction term $a_{12}$ (power and temperature) was significantly negative, indicating that combined increases in power and temperature may have antagonistic effects. In a related study, Sai-Ut et al. (2023) established a predictive model for extraction yield (EY) of longan seed extracts using distinct process parameters (ethanol concentration, temperature, and extraction time) that varied from our experimental design. Their second-order polynomial model's statistical coefficients are presented in Table 3, while Fig. 1 displays the corresponding 3D response surface plots depicting EY variations under different extraction conditions.

### 3.2 Effect of UAE factors on total phenolic contents of RTSE

Phenolic compounds, commonly present in food sources, exhibit a wide range of biological and functional benefits that play a crucial role in food quality and human health. As shown in Table 1, the total phenolic content (TPC) of RTSE varies significantly depending on ultrasonication conditions. TPC ranged from 0.008 to 0.020 mg GAE/g DW, with the maximum value also recorded in Run 23. This indicates that the optimal extraction conditions for yield also favored the recovery of phenolic compounds. Conversely, run 8 showed the lowest TPC, further supporting the notion that excessive ethanol and temperature adversely affect phenolic compound solubility and stability. The findings suggest that polar phenolic compounds are better extracted under milder conditions with higher water content in the solvent system, as water facilitates the swelling of plant material and improves compound diffusion.

The power ratio exhibited a clear influence on the total phenolic content (TPC). At the lowest power level (20%), TPC values were relatively higher in several runs. For instance, run 1 reported 0.015 ± 0.001 mg GAE/g DW, while Run 5 and Run 27 yielded 0.017 ± 0.076 mg GAE/g DW and 0.017 ± 0.044 mg GAE/g DW, respectively. In contrast, increasing the power to the highest level (X1 = + 1, 80%) often resulted in reduced TPC values. Run 2 and Run 8 showed noticeably lower TPCs of 0.013 ± 0.019 mg GAE/g DW and 0.008 ± 0.065 mg GAE/g DW, respectively reflecting decreases of 13.3% and 46.7%, respectively, compared to Run 1. This suggests that excessive power may degrade phenolic compounds, possibly due to thermal or oxidative degradation during high-energy extraction. Consistent with findings reported by Dalmau et al. (2020) for orange byproducts, comparable extraction patterns were observed for total phenolic content (TPC) across varying acoustic power densities.

Ultrasound-assisted extraction operates through two principal mechanisms: (1) transmission of ultrasonic waves and (2) cavitation effects (Ji et al. 2006). The cavitation phenomenon serves as the cornerstone of this technology, enhancing extraction efficiency through multiple physical actions. When cavitation bubbles collapse near biomass

**Table 3** Statistical indicators of the second-order polynomial model for the various response variables

| Property | Regression Coefficients of the Second-Degree Model | | | | | | | | | | | | |
|---|---|---|---|---|---|---|---|---|---|---|---|---|---|
| | $y_n = a_0 + a_1x_1 + a_2x_2 + a_3x_3 + a_4x_4 + a_{11}{x_1}^2 + a_{22}{x_2}^2 + a_{33}{x_3}^2 + a_{44}{x_4}^2 + a_{12}x_1x_2 + a_{13}x_1x_3 + a_{23}x_2x_3$ | | | | | | | | | | | | |
| | $a_0$ | $a_1$ | $a_2$ | $a_3$ | $a_4$ | $a_{11}$ | $a_{22}$ | $a_{33}$ | $a_{12}$ | $a_{13}$ | $a_{14}$ | $a_{23}$ | $R^2$ |
| **EY (%)** | 9.44* | 0.14 | 0.13 | 0.111 | 0.1233 | $-3.00\times10^{-5}$ | $6.30\times10^{-4}$ | $-1.20\times10^{-4}$ | $-3.04\times10^{-3}$* | $-1.88\times10^{-3}$ | $-4.00\times10^{-3}$ | $-3.37\times10^{-3}$ | 0.984 |
| **TPC (mg GAE/g DW)** | $4.58\times10^{-3}$* | $1.20\times10^{-4}$ | $2.53\times10^{-4}$ | $2.07\times10^{-4}$ | $5.00\times10^{-5}$ | 0.00E+00 | $-2.00\times10^{-6}$ | $-2.00\times10^{-6}$ | $-1.00\times10^{-6}$ | $-2.00\times10^{-6}$* | 0.00 | $-2.00\times10^{-6}$ | 0.989 |
| **TFC (mg QE/g DW)** | $-7.46\times10^{-2}$ | $1.79\times10^{-3}$ | $1.96\times10^{-3}$ | $1.48\times10^{-3}$ | $1.15\times10^{-4}$ | $-1.80\times10^{-5}$* | $-1.30\times10^{-5}$ | $-6.00\times10^{-6}$ | $-1.00\times10^{-6}$ | $-6.00\times10^{-6}$ | $9.00\times10^{-6}$ | $-2.30\times10^{-5}$* | 0.968 |
| **DPPH radical scavenging activity (%)** | −39.6 | 1.645* | 1.806* | 1.344* | −0.145 | $-1.38\times10^{-2}$* | $-1.49\times10^{-2}$ | $-1.24\times10^{-2}$ | $-5.04\times10^{-3}$ | $-3.71\times10^{-3}$ | $5.26\times10^{-3}$ | $-6.46\times10^{-3}$ | 0.957 |
| **FRAP Activity** | 16.75 | −0.127 | −2.30E-01 | −0.192 | $-4.08\times10^{-2}$ | $1.05\times10^{-3}$ | $1.96\times10^{-3}$ | $3.05\times10^{-3}$* | $4.98\times10^{-4}$ | $1.43\times10^{-4}$ | $-3.74\times10^{-4}$ | $3.42\times10^{-4}$ | 0.913 |

**a** The coefficients $a_0, a_1, a_2, a_3, a_4$ represent the intercept and linear terms for the independent variables $x_1$ (power ratio), $x_2$ (temperature), $x_3$ (time), and $x_4$ (ethanol concentration), respectively. The coefficients $a_{11}, a_{22}, a_{33}, a_{44}$ correspond to the quadratic terms, and $a_{12}, a_{13}, a_{14}, a_{23}$ represent the two-factor interaction terms in the second-order polynomial model (Eq. 2).

*Significant at significance level of 0.05.

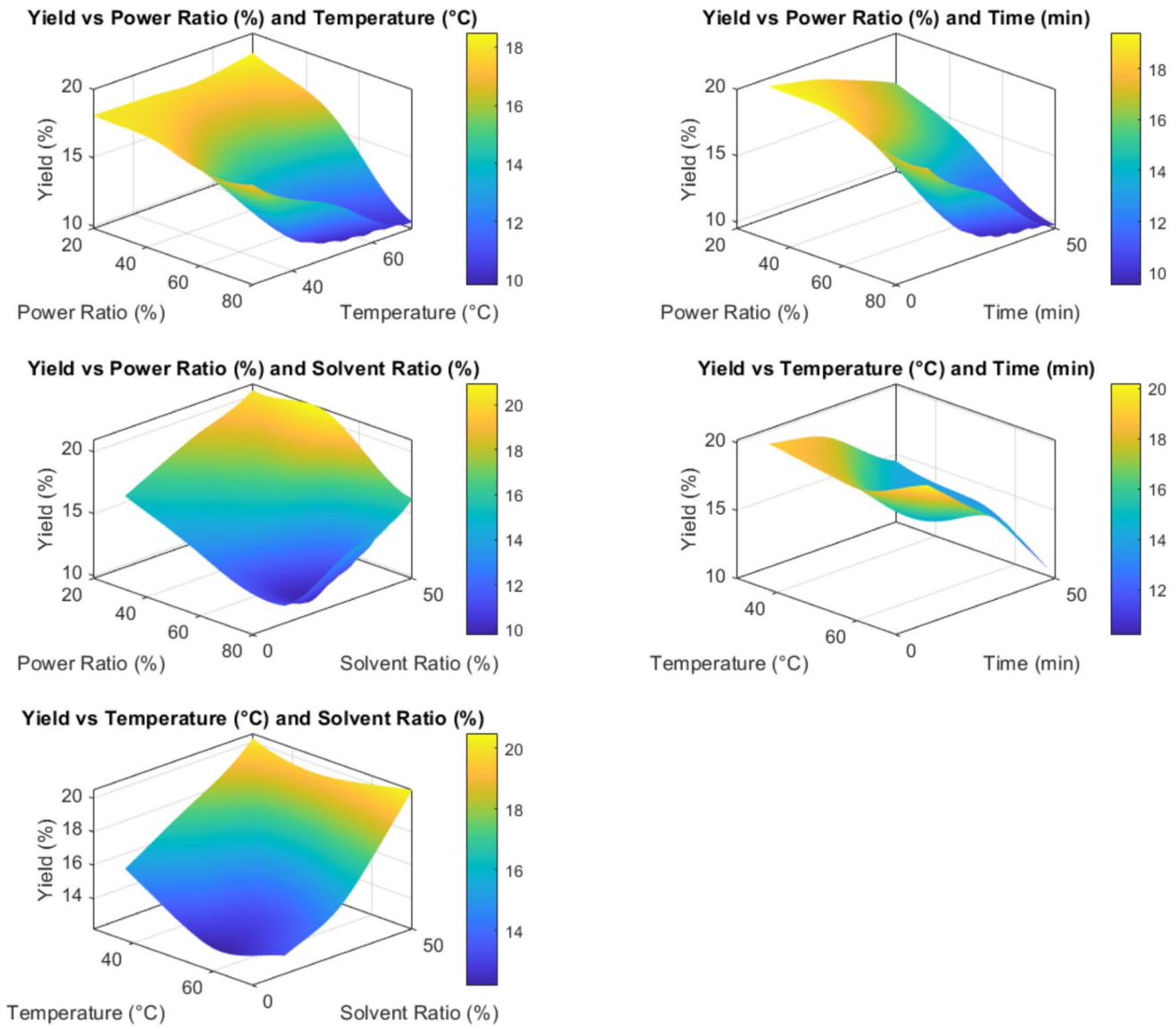



**Fig. 1** 3-D plots for the predicted values of extraction yield of RTSE in relation to the ultrasonic power ratio and exposure time using the predictive model

surfaces, they create micro-jets that mechanically disrupt cellular structures while simultaneously promoting solvent permeation into the tissue matrix (Vilkhu et al. 2008; Wen et al. 2012). These implosions generate macro-scale turbulence and particle collisions that significantly improve mass transfer by accelerating both eddy diffusion (bulk movement) and internal diffusion (molecular penetration). The combined effects of these physical processes dramatically increase interfacial contact between solvent and plant materials, explaining the superior extraction yields characteristic of ultrasonic methods.

The effect of extraction temperature on TPC was complex and intertwined with other process parameters. The data suggests that prolonged exposure to high temperature is particularly detrimental. For instance, runs at 70 °C with longer times, such as Run 12 (50 min) and Run 4 (50 min), resulted in the lowest TPC values of $0.008 \pm 0.050$ and $0.009 \pm 0.024$ mg GAE/g DW, respectively. In contrast, Run 25 (50°C, 30 min) achieved a high TPC of $0.015 \pm 0.089$ mg GAE/g DW, supporting the general benefit of moderate temperatures. However, a high TPC could also be achieved at 70 °C if the extraction time was short, as demonstrated by Run 10 (70°C, 10 min), which yielded $0.014 \pm 0.096$ mg GAE/g DW. This indicates that thermal degradation of phenolic compounds becomes significant primarily under extended thermal exposure, while short, high-temperature extraction can be effective for rapid phenolic release.

While elevated temperatures improve mass transfer efficiency by lowering solvent viscosity and enhancing cellular permeability (Dalmau et al. 2020), excessive heat (> 65 °C) promotes thermochemical degradation of phenolic compounds through oxidative reactions and molecular interactions with other matrix components (Durling et al. 2007; Sai-Ut et al. 2023). This creates a critical trade-off in extraction optimization—whereas moderate heating facilitates solvent penetration and compound solubility, supraoptimal temperatures compromise phenolic stability through multiple degradation pathways.

The effect of extraction time was also evident. Shorter extraction times (10 min) generally produced higher TPC values in combination with other optimized conditions. For example, run 5 (10 min) yielded 0.017 ± 0.076 mg GAE/g DW, while Run 10 (10 min) reached a high TPC of 0.014 ± 0.096 mg GAE/g DW. On the contrary, longer extraction times (50 min) tended to decrease TPC, as observed in Run 12 and Run 8, which showed TPCs of 0.008 ± 0.050 mg GAE/g DW and 0.008 ± 0.065 mg GAE/g DW, respectively. This suggests that prolonged exposure may lead to the degradation of phenolic compounds or equilibrium being reached early in the process.

Ethanol concentration had a relatively minor yet noticeable effect on TPC. At the central level (30%), most runs yielded consistent and moderate-to-high TPC values, such as Run 10 (0.014 ± 0.096 mg GAE/g DW) and Run 25 (0.015 ± 0.089 mg GAE/g DW). However, deviations from this concentration slightly affected phenolic recovery. For example, run 13 (10%) had a TPC of 0.013 ± 0.109 mg GAE/g DW, while Run 24 (50%) had a TPC of 0.014 ± 0.025 mg GAE/g DW, suggesting a ~ 7.1% decrease. These results imply that moderate ethanol levels (around 25%) are optimal for extracting phenolic compounds, possibly due to balanced polarity matching between the solvent and phenolic compounds.

### 3.3 Effect of UAE factors on total flavonoid contents

The analysis of total flavonoid content (TFC) across various ultrasonication conditions demonstrated notable variability (Table 1). The TFC showed a distinct pattern, ranging from 0.007 to 0.049 mg QE/g DW. The highest TFC was obtained in Run 10, which involved extraction at 70 °C for 10 min using 30% ethanol. This result suggests that a shortest extraction time benefits flavonoid release, particularly under aqueous conditions. In contrast, lower TFC values were observed in runs using longer extraction times, such as run 8 and run 12 (50 min, 30% ethanol), implying that prolonged ultrasonication leads to the degradation of flavonoid compounds.

The power ratio exerted a significant effect on the total flavonoid content (TFC). Lower power settings, specifically at 20%, consistently resulted in higher TFC values across several experimental runs. For example, run 10 recorded the highest TFC of 0.049 ± 0.0064 mg QE/g DW, while Runs 5 and 27, also conducted at this low power level, showed TFC values of 0.024 ± 0.0010 mg QE/g DW and 0.046 ± 0.0002 mg QE/g DW, respectively. In contrast, increasing the power ratio to 80% led to a marked reduction in flavonoid content, as seen in Run 2 (0.020 ± 0.0003 mg QE/g DW) and Run 8 (0.015 ± 0.0016 mg QE/g DW). This decrease at higher power intensities likely reflects flavonoid degradation caused by excessive cavitation and localized heating.

Similarly, extraction temperature played a crucial role in determining TFC, with its effect being highly dependent on the extraction time. High yields could be achieved at 70 °C, but only when the exposure time was limited. This is demonstrated by the high TFC values in Run 10 (70°C, 10 min) at 0.049 ± 0.0064 mg QE/g DW and Run 27 (70°C, 30 min) at 0.046 ± 0.0002 mg QE/g DW. However, when a high temperature of 70 °C was combined with a prolonged extraction time of 50 min, a significant decline in TFC was observed, as seen in Run 4 and Run 12, which yielded only 0.013 ± 0.0013 and 0.013 ± 0.0026 mg QE/g DW, respectively. These findings suggest that the thermal degradation of flavonoid compounds becomes significant primarily under extended exposure to high temperatures.

Extraction time also influenced TFC, with shorter durations being more favorable. Runs with a 10-min extraction time, such as run 10 and run 5, showed relatively high TFC levels of 0.049 ± 0.0064 mg QE/g DW and 0.024 ± 0.0010 mg QE/g DW, respectively. Conversely, longer extraction times, exemplified by Run 12 with a 50-min duration, yielded lower TFC (0.013 ± 0.0026 mg QE/g DW). This decline may be attributed to oxidative degradation or saturation effects occurring during prolonged extraction periods. The temperature-dependent behavior of total flavonoid content (TFC) aligns with findings reported for Ruby S apple peel (Park et al. 2022) and orange byproduct extracts (Dalmau et al. 2020), suggesting a consistent thermal sensitivity of flavonoids across different plant matrices.

Finally, ethanol concentration affected flavonoid extraction efficiency in a non-linear manner. Moderate ethanol concentrations of 30% proved optimal, with Runs 10 and 25 recording TFC values of 0.049 ± 0.0064 mg QE/g DW and 0.037 ± 0.0020 mg QE/g DW, respectively. In comparison, both lower (10%) and higher (50%) ethanol concentrations resulted in decreased TFC, as seen in Run 13 (0.020 ± 0.0031 mg QE/g DW) and Run 24 (0.017 ± 0.0035 mg QE/g DW). This trend implies that extreme solvent polarities may negatively impact flavonoid solubility and extraction efficiency.

### 3.4 Effect of UAE Factors on DPPH radical scavenging activity

Antioxidant activity, as assessed by DPPH radical scavenging activity, ranged from 27.13% to 63.16%. The highest value was observed in run 25 (50 °C, 50 min, 30% ethanol, 30 mL/g), a condition close to the center point of the design. Although Run 23 exhibited high DPPH activity (61.48%), run 25 slightly surpassed it, indicating that antioxidant activity is not entirely dependent on TPC or TFC but may also be influenced by the presence and interaction of other antioxidant constituents. In contrast, the lowest activity was recorded in Run 23 (50 °C, 10 min, 50% ethanol) at 27.13 ± 5.59%, indicating that high ethanol concentration combined with short extraction time may limit the release of radical-scavenging compounds. Although Run 23 also showed high extraction yield, its low DPPH activity suggests that antioxidant potential is not solely dependent on extract mass but on the specific composition of bioactive compounds. Run 4 (70 °C, 30 min, 10% ethanol) also exhibited reduced activity (43.09 ± 3.12%), likely due to thermal degradation under prolonged high-temperature exposure.

The power ratio showed a significant impact on DPPH scavenging activity. The maximum power level (80%) frequently led to diminished scavenging, as evidenced in run 8 (49.13 ± 5.02%) and run 26 (38.03 ± 2.29%). Conversely, robust antioxidant activity was often attained at low (20%) and moderate (50%) power levels. For instance, run 10 (50% power) and run 27 (20% power) exhibited significant inhibition percentages of 52.59 ± 2.31% and 45.37 ± 6.60%, respectively. This indicates that high power may result in the deterioration of antioxidant molecules.

The extraction temperature significantly influenced antioxidant activity, with moderate temperatures typically enhancing it. At 50 °C, DPPH inhibition reached its highest point in Run 25 (63.16 ± 3.14%) and was notably robust in Run 10 (52.59 ± 2.31%). In contrast, the maximum temperature (70°C) frequently resulted in diminished activity, as evidenced in run 4 (43.09 ± 3.12%) and run 12 (53.58 ± 1.19%), corroborating the concept of thermal instability for certain antioxidants. The concentration of ethanol was a critical variable, with the optimal amount (30%) demonstrating the highest reliability for attaining elevated DPPH activity. Runs 25 and 10, both utilizing 30% ethanol, produced inhibition rates of 63.16% and 52.59%, respectively. Variations from this concentration, especially an increase to 50% ethanol, frequently led to more variability and occasionally reduced activity, as evidenced in Run 24 (55.78 ± 8.20%). This highlights the significance of balanced solvent polarity for the effective extraction of radical-scavenging chemicals. Similar effects on antioxidant activity have been observed in studies on orange byproduct extract (Dalmau et al. 2020), Ruby S apple peel (Park et al. 2022) and almond by-products (Prgomet et al. 2019).

### 3.5 Effect of UAE factors on ferric reducing antioxidant power

The FRAP values ranged from 3.71 to 6.36, with the highest observed in Run 12 (50 °C, 50 min, 50% ethanol, 30 mL/g). These conditions, although suboptimal for TPC and TFC, appear favorable for extracting compounds with strong reducing capacity, possibly less polar antioxidants that require a higher ethanol content for solubilization. In contrast, the lowest FRAP values were recorded in Run 19 (3.71 ± 0.09) and Run 15 (3.72 ± 0.13), both involving 50% ethanol but differing in other parameters, indicating complex interactions between extraction conditions.

Ultrasonic power showed variable effects on FRAP. Moderate power (50% in Run 25 and run 12) yielded a high value (6.00 ± 0.28 mmol $Fe^{2+}$/g DW and 6.36 ± 0.36 mmol $Fe^{2+}$/g DW, respectively), but high power (80% in Run 8) also produced appreciable activity (6.05 ± 0.45 mmol $Fe^{2+}$/g DW). This suggests that FRAP-active compounds are not uniformly degraded by ultrasound within the tested range, and the effect of power depends on its interaction with other parameters.

Temperature effects were non-linear. Although 70 °C in Run 12 gave the highest FRAP (6.36 ± 0.36 mmol $Fe^{2+}$/g DW), other runs at 70 °C (Run 4: 5.21 ± 1.40 mmol $Fe^{2+}$/g DW) showed reduced activity. Similarly, 50 °C produced both high (Run 25: 6.00 ± 0.28 mmol $Fe^{2+}$/g DW) and moderate (Run 10: 5.33 ± 0.14 mmol $Fe^{2+}$/g DW) values. This indicates thermal effects depend strongly on interactions with time and ethanol concentration rather than temperature alone.

Extraction time displayed complex behavior. Both short (Run 10: 10 min, 5.33 ± 0.14 mmol $Fe^{2+}$/g DW) and long durations (Run 12: 50 min, 6.36 ± 0.36 mmol $Fe^{2+}$/g DW) could yield significant FRAP values. The optimal extraction time for maximizing reducing capacity appears to depend on simultaneous optimization of temperature and ethanol concentration.

Ethanol concentration played a critical and non-linear role in determining FRAP outcomes, reflecting the polarity-dependent solubility of electron-donating antioxidants.

The highest FRAP activity was observed at 50% ethanol (Run 12: 6.36 ± 0.36 mmol $Fe^{2+}$/g DW), suggesting that a balanced hydrophilic–lipophilic solvent system efficiently extracts redox-active phenolics with intermediate polarity such as certain flavonoid aglycones and phenolic acids—that are strong ferric reductants. Although 30% ethanol also supported high activity in some runs (e.g., Run 25: 6.00 ± 0.28 mmol $Fe^{2+}$/g DW), the same concentration yielded lower values in others (e.g., Run 10: 5.33 ± 0.14 mmol $Fe^{2+}$/g DW),

indicating that ethanol's effect is contingent upon temperature and time. Conversely, both lower (10%) and higher (50%) ethanol levels in certain conditions diminished reducing power (e.g., Run 24: $4.13 \pm 0.30$ mmol $Fe^{2+}$/g DW at 50% ethanol), likely because highly aqueous solvents poorly solubilize less-polar reductants, while highly ethanolic mixtures may inadequately extract more polar, hydroxyl-rich phenolics. Similar effects on antioxidant activity have been observed in studies on orange byproduct extract (Dalmau et al. 2020), Ruby S apple peel (Park et al. 2022) and almond by-products (Prgomet et al. 2019).

The different redox processes of each assay are the cause of the observed differences between FRAP results and total phenolic or flavonoid concentrations. Certain structural elements, such as ortho-dihydroxyl groups (catechol moieties) and conjugation systems in phenolic compounds, have a significant impact on the electron-transfer capacity measured by FRAP (Prior et al. 2005). Flavonoids having monohydroxylated rings, like kaempferol, have a lower reducing power than those with catechol B-rings, like quercetin derivatives (Mutha et al. 2021). Therefore, if the flavonoids present have poor substitution patterns or are glycosylated, which can lower electron-donating ability, a high TFC may not be correlated with a high FRAP (Xiao et al. 2021).

Moreover, DPPH detects both electron and hydrogen-atom transfer, while FRAP mainly records the activity of chemicals that act by electron transfer. FRAP is frequently more significantly influenced by phenolic acids and aglycones than by glycosylated flavonoids (Shahidi and Samarasinghe 2025). This is supported by the LC-QTOF-MS profile's inclusion of galloyl and caffeoyl derivatives, which are strong ferric ion reducers (Bodoira and Maestri 2020).

### 3.6 Analysis of variance and model interpretation

The ANOVA results (Table 2) revealed significant overall regression models for EY, TPC, TDC, DPPH and FRAP, indicating these models effectively describe the relationships between extraction parameters and responses. For EY, while individual linear effects of power ratio ($X_1$) and temperature ($X_2$) were statistically insignificant ($p > 0.05$), their interaction term ($X_1X_2$) showed strong significance ($F = 12.68$, $p = 0.038$). This finding is supported by the substantial negative coefficient ($-3.04 \times 10^{-3}$) in the polynomial model (Table 3), demonstrating that simultaneous increases in power (> 60%) and temperature (> 50 °C) adversely affect yield. The ethanol concentration ($X_4$) emerged as the most influential individual parameter for EY ($F = 5.21$, $p = 0.107$), with no significant quadratic effects observed, suggesting relatively broad optimal ranges for process parameters.

The extraction of phenolic compounds showed distinct behavior, with temperature ($X_2$) exhibiting the strongest positive linear effect (coefficient $2.53 \times 10^{-}4$ in Table 3). The significant power-time interaction ($X_1X_3$; $F = 17.13$, $p = 0.026$) indicates that prolonged extraction at higher power levels enhances phenolic recovery. Notably, the absence of significant quadratic terms suggests linear scalability of TPC with parameter increases. In contrast, total flavonoid content (TFC) demonstrated more complex behavior, with significant quadratic effects for power ratio ($X_1^2$; $F = 10.49$, $p = 0.048$) and a crucial temperature–time interaction ($X_2X_3$; $F = 18.37$, $p = 0.023$). These results imply that flavonoid extraction requires careful balancing of parameters, particularly avoiding excessive power (> 60%) while optimizing the temperature–time combination.

DPPH radical scavenging activity showed significant linear effects for power, temperature, and time, with particularly strong influence from power ratio ($F = 31.99$, $p = 0.011$). The significant quadratic power effect ($X_1^2$; $F = 23.15$, $p = 0.017$) confirms the degradation of antioxidant compounds at power levels exceeding 70%. Interestingly, FRAP activity displayed different behavior, with a significant quadratic time effect ($X_3^2$; $F = 10.45$, $p = 0.048$) suggesting optimal extraction between 30–50 min. The negative linear coefficients for FRAP activity indicate that conventional parameter increases may adversely affect this antioxidant measure, potentially due to the degradation of specific reducing compounds at higher extraction intensities.

A predictive model was previously developed by Sai-Ut et al. (2023) and Fikry et al. (2024b) to estimate the phytochemical characteristics of longan seed extract, utilizing extraction parameters such as ethanol concentration, extraction temperature, and time. These parameters differ from those applied in the present study, which focused on optimizing UAE conditions. Moreover, Figs. 1, 2, 3, 4, 5 present the three-dimensional response surface plots for extraction yield (EY), total phenolic content (TPC), total flavonoid content (TFC), DPPH radical scavenging activity, and FRAP activity of RTSE, as predicted by the developed models. These response surfaces effectively illustrate the influence of various extraction conditions on each response variable.

### 3.7 Determination of optimum conditions of UAE process

Identifying the optimal conditions for the UAE process is essential to minimize the degradation of sensitive food compounds, thereby preserving overall quality. To achieve this, an optimization procedure was carried out to enhance extraction yield along with the recovery of total phenolic content (TPC), total flavonoid content (TFC), DPPH radical scavenging activity, and FRAP activity during conventional solvent extraction (RTSE). Second-order polynomial models developed in this study were employed to estimate the most effective extraction conditions and simultaneously predict optimal responses for the five target variables.

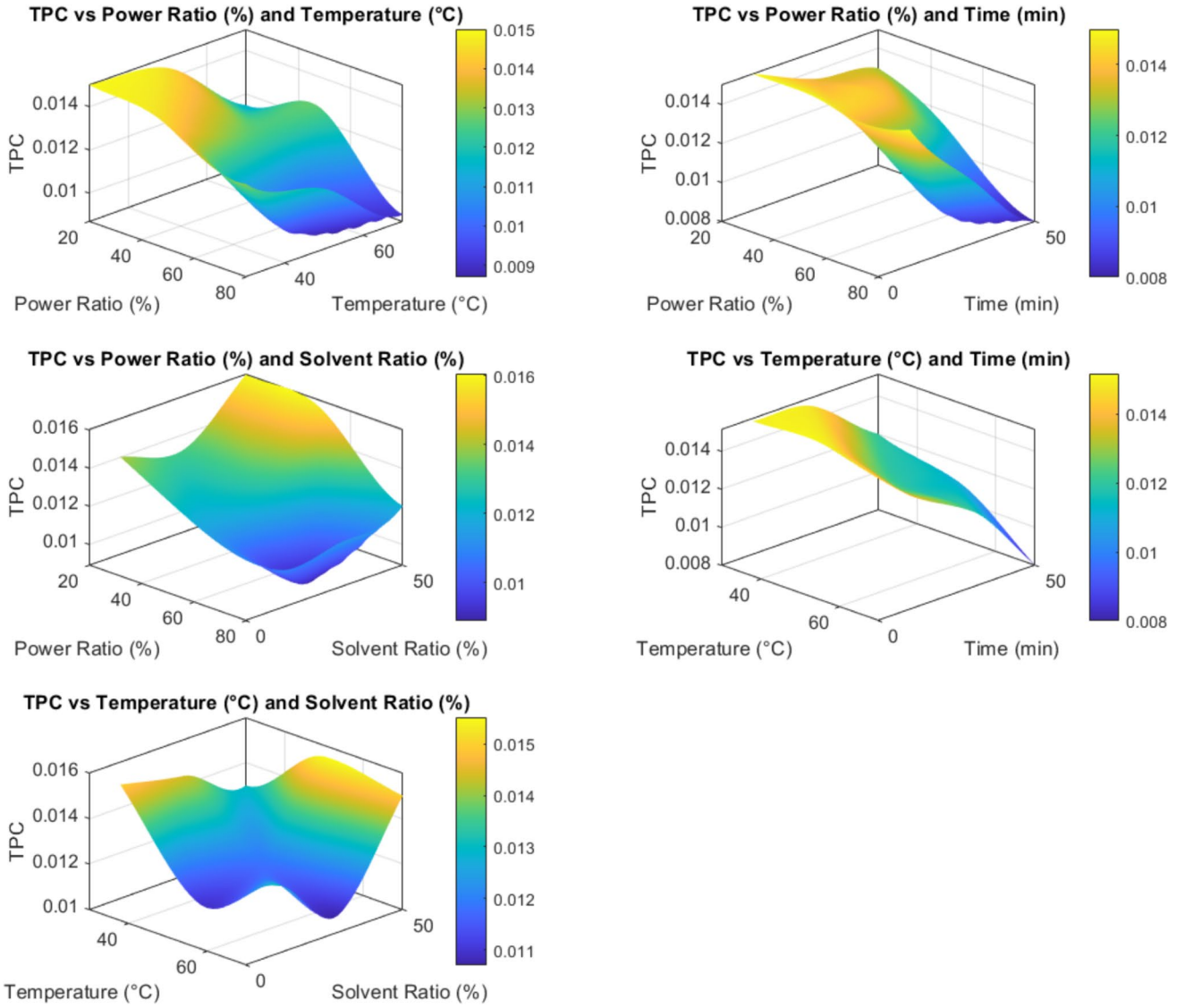



**Fig. 2** 3-D plots for the predicted values of FRAP of RTSE in relation to the ultrasonic power ratio and exposure time using the predictive model

The optimal region was established by superimposing and interpreting the contour plots generated under the defined constraints. As a result, the ideal extraction parameters were determined to be an ultrasonic power ratio of 44%, extraction temperature of 60 °C, extraction time of 10 min, and solvent (ethanol) concentration of 23%. These conditions were then used to conduct RTSE trials expected to yield maximized responses within the specified optimization boundaries. The predicted values under these optimal conditions are summarized in Table 4.

To validate the accuracy and reliability of the developed models, experimental trials were conducted under the optimized RTSE conditions (power ratio 44%, temperature 60 °C, extraction time 10 min, and ethanol concentration 23%). The experimental outcomes were then compared with the model-predicted values across all studied responses.

For extraction yield (EY), the experimental value was $17.36 \pm 0.08\%$, slightly lower than the predicted value of 18.61%. The 95% confidence intervals shown in Table 4 were derived from the prediction intervals of the respective second-order polynomial models, representing the range within which the true mean response is expected to lie with 95% probability, given the model uncertainty and experimental error estimated from center-point replicates. Nonetheless, the observed value fell within the 95% confidence interval (15.729–21.495), indicating acceptable model accuracy and good prediction capability. A similar trend was noted for total phenolic content (TPC), where the experimental value ($0.0147 \pm 0.001$ mg GAE/g DW) closely matched

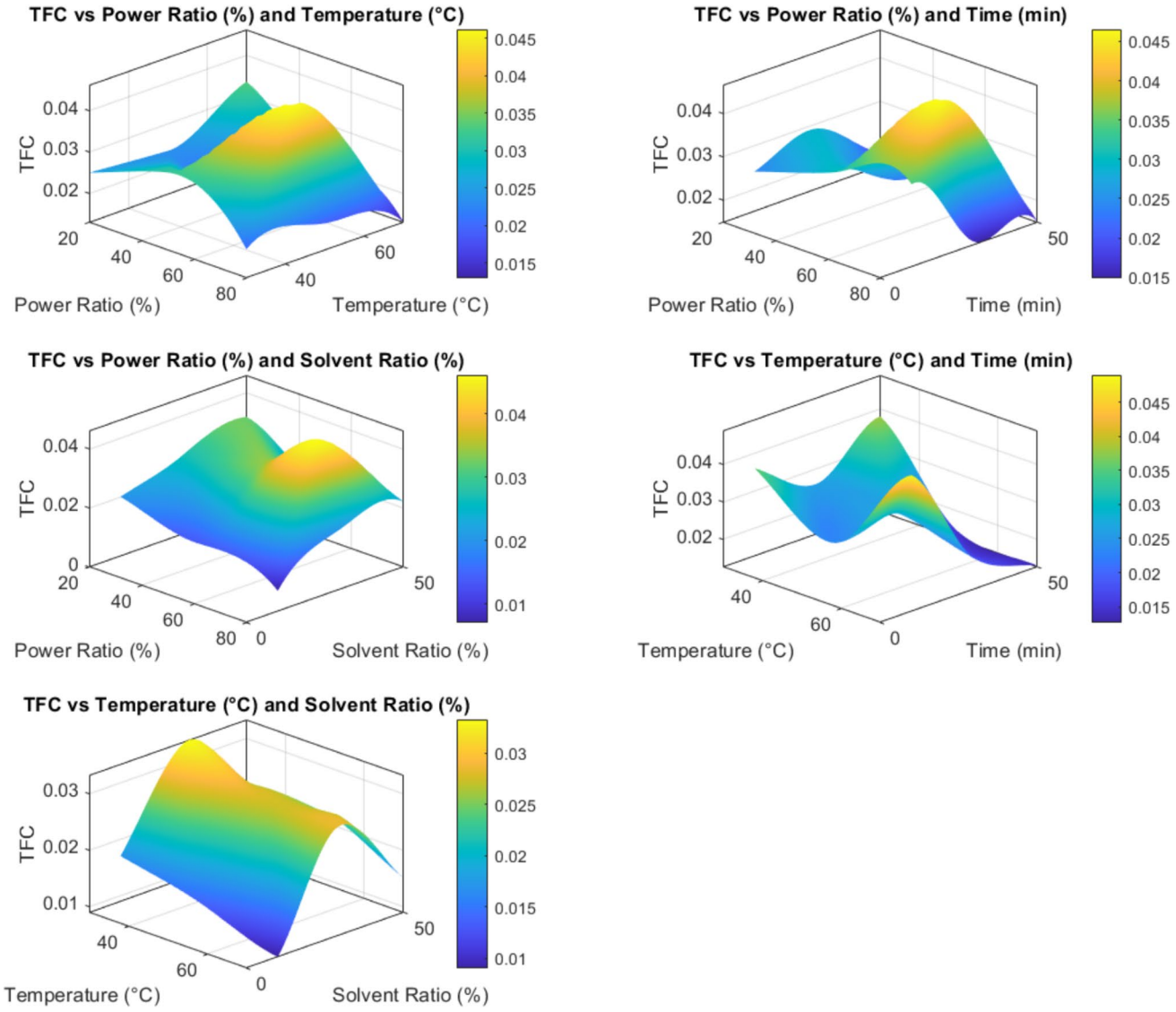



**Fig. 3** 3-D plots for the predicted values of TPC of RTSE in relation to the ultrasonic power ratio and exposure time using the predictive model

the predicted value (0.015 mg GAE/g DW), and was well contained within the confidence bounds (0.0130–0.0165).

Interestingly, total flavonoid content (TFC) showed a slightly higher experimental value (0.033 ± 0.003 mg QE/g DW) than the predicted value (0.044 mg QE/g DW). Despite this deviation, the experimental outcome remained within the 95% CI (0.0315–0.0561), suggesting that the model slightly underestimated flavonoid recovery under these conditions.

For antioxidant activity, the DPPH radical scavenging assay showed high alignment between predicted (56.10%) and experimental (60.44 ± 1.70%) values, again lying comfortably within the confidence range (49.89–62.30%). This confirms the robustness of the model in estimating antioxidant performance. However, FRAP activity displayed a more noticeable discrepancy: the experimental value (5.97 ± 0.033 mmol $Fe^{2+}$/g DW) was lower than the predicted value (5.13), though still within the broader 95% confidence interval (3.999–6.266). This may reflect the higher variability and complexity of redox-dependent antioxidant reactions compared to radical-scavenging mechanisms like DPPH. The optimal conditions identified in this study may be comparable to those reported for longan seeds by Sai-Ut et al. (2023).

### 3.8 LC-QTOF-MS Profile of the optimized RTSE

LC-QTOF-MS profiling in positive and negative modes revealed a metabolome dominated by flavonoid glycosides and phenolic esters, supported by isoflavones, oxylipins,

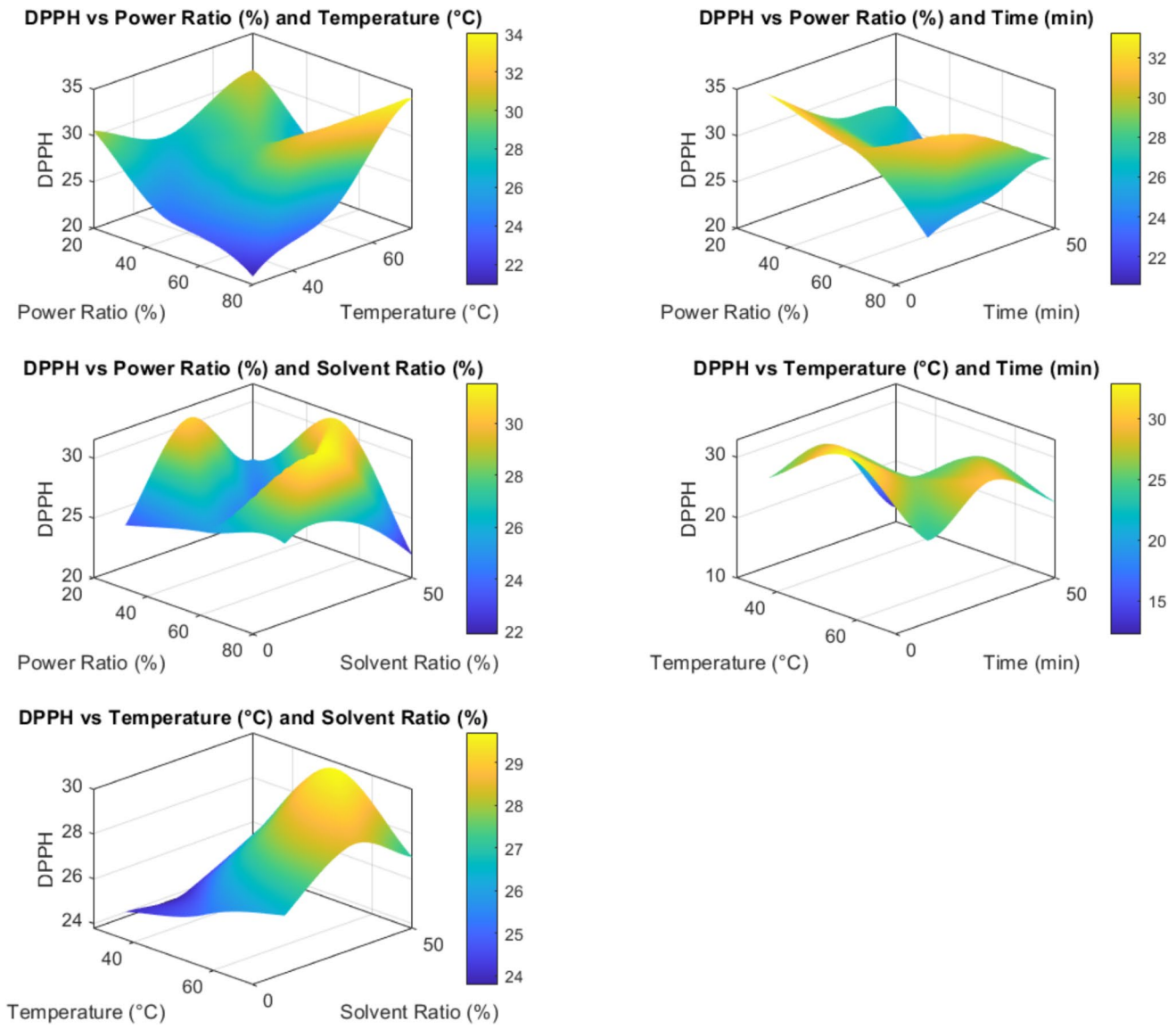



**Fig. 4** 3-D plots for the predicted values of TFC of RTSE in relation to the ultrasonic power ratio and exposure time using the predictive model

megastigmane glycosides, and a late-eluting glycolipid. In the negative mode (Table 5), 32 compounds were identified. Major flavonoids included quercetin 3-O-gentiobioside (m/z 626.1470, RT 16.524 min) confirmed by MS/MS to the quercetin aglycone, and herbacetin 8-rhamnoside (m/z 448.1003, RT 17.048 min). We also observed a luteolin-type C-glycoside (6-C-xylosylluteolin 2″-O-rhamnoside; m/z 564.1481, RT 16.743 min) with characteristic cross-ring fragments. Additional mid-polarity flavonoids comprised herbacetin-7-methyl ether 3-(2″-(E)-feruloylglucoside) (m/z 654.1591, RT 17.294 min) and the isoflavone orobol 8-C-(6″-acetylglucoside) (m/z 490.1112, RT 17.578 min). Early eluting phenolic esters and small phenolics were abundant including 6-O-galloyl-D-glucose (m/z 332.0743, RT 3.136 min) and 3-O-caffeoyl-4-O-methylquinic acid (m/z 368.1092, RT 1.784 min) displayed the expected MS/MS ions of gallate/quinic/caffeate. Later retention times featured oxylipins, e.g., 11,12,13-trihydroxy-9-octadecenoic acid (m/z 330.2396, RT 18.435 min) and 9,12,13-trihydroxy-10,15-octadecadienoic acid (m/z 328.2238, RT 18.607 min), alongside 3,12-dihydroxyhexadecanoic acid (m/z 288.2296, RT 18.654 min). In addition, 12 identified compounds were detected in the positive mode (Table 6). Kaempferol 7-O-glucoside (m/z 448.1031, RT 16.893 min) was confirmed by the neutral loss of 162 Da to m/z 287. Plant hormone conjugates were also present, including abscisic alcohol 11-glucoside (m/z 412.2099, RT 11.895 min) and cis-zeatin 9-glucoside (m/z 381.1656, RT 5.827 min).

The LC-QTOF-MS dataset provides strong evidence that the antioxidant activity of the crude extract is primarily

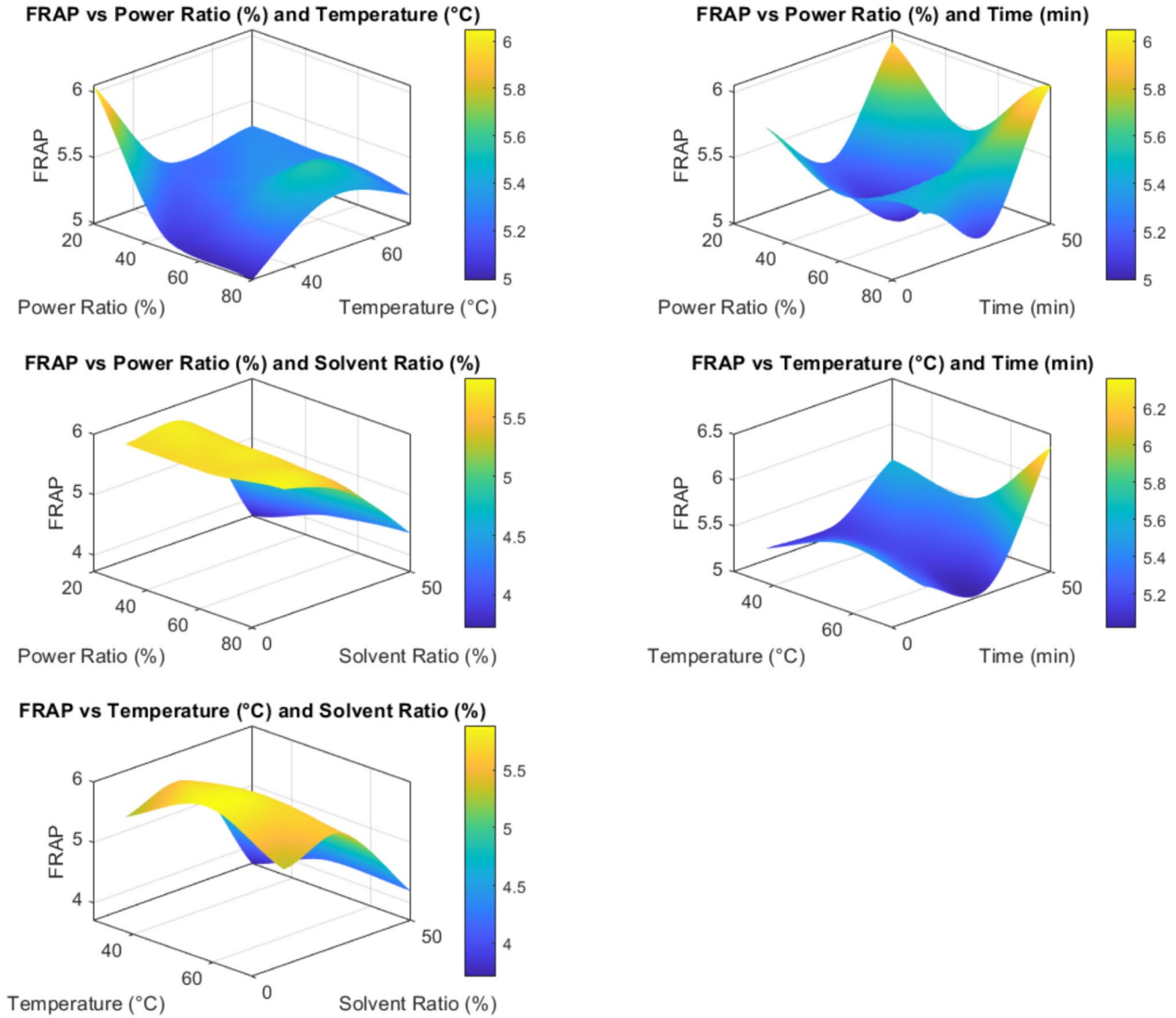



**Fig. 5** 3-D plots for the predicted values of DPPH of RTSE in relation to the ultrasonic power ratio and exposure time using the predictive model

**Table 4** Experimental results and model predictions for RTSE at the optimized parameters (power ratio of 44%, 60 C, 10 min and solvent ratio of 23%)

| Response | Predicted values | Experimental values | 95% CI* |
|---|---|---|---|
| EY (%) | 18.61 | 17.36 ± 0.08 | (15.729, 21.495) |
| TPC (mg GAE/g DW) | 0.015 | 0.0147 ± 0.001 | (0.013043, 0.016471) |
| TFC (mg QE/g DW) | 0.044 | 0.033 ± 0.003 | (0.03147, 0.05609) |
| % DPPH Radical Scavenging Activity | 56.10 | 60.44 ± 1.70 | (49.89, 62.30) |
| FRAP Activity (mmol $Fe^{2+}$/g DW) | 5.13 | 5.97 ± 0.033 | (3.999, 6.266) |

* Confidence intervals at level of 0.05

attributed to a cluster of polyphenolic flavonoid glycosides and phenolic esters, while non-phenolic metabolites such as oxylipins (Savchenko et al. 2022), megastigmane glycosides (Bao et al. 2017), and phytohormone conjugates (Khan et al. 2018) play only secondary roles. Several flavonoid glycosides were confidently identified, including quercetin 3-O-gentiobioside, luteolin 7-gentiobioside, herbacetin 7-methyl ether 3-(2"-(E)-feruloylglucoside), and kaempferol 7-O-glucoside. Their MS/MS spectra displayed characteristic neutral losses of 162 Da (hexose) and 146 Da (rhamnose),

**Table 5** LC-QTOF-MS identified compounds of RTSE in the negative mode (optimized UAE conditions: 44% power, 60 °C, 10 min, 23% ethanol)

| | Name | Cpd | Hits | Diff (DB, ppm) | Formula | Mass | Score | RT | Score (MFE) |
|---|---|---|---|---|---|---|---|---|---|
| 1 | 13-Hydroxyoctadeca-9,11-dienoic acid | 920 | 95 | −0.58 | $C_{18}H_{32}O_3$ | 296.235 | 98.57 | 21.472 | 84.6 |
| 2 | Tuberonic acid | 853 | 93 | −2.16 | $C_{12}H_{18}O_4$ | 226.12 | 77.24 | 18.196 | 100 |
| 3 | Nardoguaianone J | 925 | 92 | −1.4 | $C_{15}H_{22}O_2$ | 234.1617 | 86.25 | 21.536 | 85.7 |
| 4 | Luteolin 7-gentiobioside | 769 | 90 | 0.71 | $C_{27}H_{30}O_{16}$ | 610.1538 | 97.77 | 16.787 | 100 |
| 5 | 8-C-Galactosylluteolin | 727 | 85 | −1.63 | $C_{21}H_{20}O_{11}$ | 448.0998 | 69.37 | 16.541 | 80 |
| 6 | D-Manno-2-Heptulose | 143 | 81 | −0.91 | $C_7H_{14}O_7$ | 210.0738 | 99.59 | 1.815 | 100 |
| 7 | Farformolide B | 892 | 78 | −1.1 | $C_{17}H_{26}O_5$ | 310.1777 | 84.94 | 20.065 | 99.3 |
| 8 | Herbacetin 8-rhamnoside | 812 | 77 | −0.58 | $C_{21}H_{20}O_{11}$ | 448.1003 | 99.7 | 17.048 | 100 |
| 9 | Digalactosyl ononitol | 140 | 71 | 2.55 | $C_{19}H_{34}O_{18}$ | 550.1759 | 64.99 | 1.808 | 84.2 |
| 10 | Erlose | 256 | 71 | −1.17 | $C_{18}H_{32}O_{16}$ | 504.1684 | 89.02 | 2.025 | 100 |
| 11 | 3,12-Dihydroxyhexadecanoic acid | 863 | 71 | −1.54 | $C_{16}H_{32}O_4$ | 288.2296 | 98.83 | 18.654 | 100 |
| 12 | 4-Hydroxy-5-[2-[(E)−3-hydroxyprop-1-enyl]−4-methylphenyl]−3-methylhexan-2-one | 907 | 70 | −3.36 | $C_{17}H_{24}O_3$ | 276.1716 | 80.43 | 20.862 | 82 |
| 13 | 6-C-Xylosylluteolin 2"-O-rhamnoside | 753 | 67 | 0.31 | $C_{26}H_{28}O_{14}$ | 564.1481 | 95.4 | 16.743 | 80 |
| 14 | Quercetin 3-O-gentobioside | 726 | 64 | −2.12 | $C_{27}H_{30}O_{17}$ | 626.147 | 96.2 | 16.524 | 100 |
| 15 | 11,12,13-trihydroxy-9-octadecenoic acid | 859 | 62 | −3.17 | $C_{18}H_{34}O_5$ | 330.2396 | 81.75 | 18.435 | 100 |
| 16 | 5a,6a-Epoxy-7E-megastigmene-3b,9e-diol 9-glucoside | 801 | 53 | 1.37 | $C_{19}H_{32}O_8$ | 388.2103 | 81 | 16.98 | 97.8 |
| 17 | Corchoionoside A | 628 | 53 | −0.34 | $C_{19}H_{32}O_8$ | 388.2096 | 77.81 | 11.647 | 97.7 |
| 18 | Orobol 8-C-(6"-acetylglucoside) | 843 | 52 | 0.14 | $C_{23}H_{22}O_{12}$ | 490.1112 | 97.62 | 17.578 | 100 |
| 19 | Gluconic acid | 88 | 50 | −2.01 | $C_6H_{12}O_7$ | 196.0579 | 99.21 | 1.72 | 100 |
| 20 | Cinnacasside B | 710 | 41 | −2.72 | $C_{25}H_{36}O_{11}$ | 512.2244 | 66.21 | 16.433 | 100 |
| 21 | Phloionolic acid | 878 | 45 | −2.4 | $C_{18}H_{36}O_5$ | 332.2555 | 83.16 | 19.461 | 88.6 |
| 22 | Fagopyritol A3 | 196 | 38 | −1.99 | $C_{24}H_{42}O_{21}$ | 666.2205 | 45.13 | 1.888 | 80 |
| 23 | Herbacetin 7-methyl ether 3-(2"-(E)-feruloylglucoside) | 833 | 37 | 1.03 | $C_{32}H_{30}O_{15}$ | 654.1591 | 97.11 | 17.294 | 100 |
| 24 | Dihydroferulic acid 4-O-glucuronide | 642 | 35 | 1.35 | $C_{16}H_{20}O_{10}$ | 372.1062 | 82.7 | 12.88 | 93.2 |
| 25 | Swertiapunimarin | 584 | 35 | −1.82 | $C_{22}H_{32}O_{14}$ | 520.1783 | 97.57 | 9.049 | 84.4 |
| 26 | 9,12,13-trihydroxy-10,15-octadecadienoic acid | 862 | 30 | −3.54 | $C_{18}H_{32}O_5$ | 328.2238 | 80.17 | 18.607 | 100 |
| 27 | 6-O-Galloyl-D-glucose | 479 | 23 | −0.03 | $C_{13}H_{16}O_{10}$ | 332.0743 | 73.17 | 3.136 | 100 |
| 28 | Aquilide A | 548 | 22 | −1.91 | $C_{20}H_{30}O_8$ | 398.1933 | 83.04 | 7.141 | 99.3 |
| 29 | 3-O-Caffeoyl-4-O-methylquinic acid | 132 | 22 | −4.11 | $C_{17}H_{20}O_9$ | 368.1092 | 55.59 | 1.784 | 100 |
| 30 | 7-O-Galloylsilybin | 373 | 17 | −0.97 | $C_{32}H_{26}O_{14}$ | 634.1316 | 72.14 | 2.445 | 92.4 |
| 31 | Puerarin 6"-O-xyloside | 835 | 16 | −1.04 | $C_{26}H_{28}O_{13}$ | 548.1524 | 93.69 | 17.37 | 100 |
| 32 | Feruloyl arabinobiose | 599 | 15 | 0.11 | $C_{20}H_{26}O_{12}$ | 458.1425 | 76.96 | 9.97 | 82.8 |

producing aglycone fragment ions at m/z 301 (quercetin/herbacetin) and m/z 287 (kaempferol/luteolin). These fragmentation behaviors, combined with precise mass accuracy and consistent retention times, provide high confidence for their annotation. Structurally, these flavonoids share common antioxidant motifs, including a catechol B-ring, a C2 = C3 double bond conjugated with a 4-oxo group, and hydroxyl groups at C3 and C5, which are well documented to enhance electron donation, hydrogen atom transfer, and metal chelation (Jacob et al. 2011). Quercetin- and herbacetin-derived glycosides, which contain a catechol B-ring, are generally more potent than kaempferol analogues (Olennikov and Prokopyev 2024). The coexistence of O- and C-glycosides is particularly noteworthy. O-glycosides such as quercetin 3-O-gentiobioside (Novaes et al. 2019) and kaempferol 7-O-glucoside (Wang et al. 2018) are enzymatically hydrolyzable, releasing aglycones with high antioxidant activity, whereas C-glycosides such as 6-C-xylosylluteolin 2"-O-rhamnoside are more resistant to enzymatic cleavage and remain stable during metabolism. This dual presence suggests a synergistic contribution, O-glycosides provide rapid antioxidant responses through aglycone release (Xie et al. 2022), while C-glycosides act as longer-lasting antioxidant reservoirs due to their metabolic stability (Gurib-Fakim 2006). Such complementary behavior has been recognized in natural product chemistry as an important factor underlying

**Table 6** LC-QTOF identified compounds of RTSE in the positive mode (optimized UAE conditions: 44% power, 60 °C, 10 min, 23% ethanol)

| | Name | Cpd | Hits | Diff (DB, ppm) | Formula | Mass | Score | RT | Score (MFE) |
|---|---|---|---|---|---|---|---|---|---|
| 1 | Manghaslin | 377 | 62 | 3.49 | $C_{33}H_{40}O_{20}$ | 756.2139 | 92.19 | 13.008 | 100 |
| 2 | 3-(3-Hydroxyphenyl)propanoic acid | 583 | 61 | 4.34 | $C_9H_{10}O_3$ | 166.0637 | 81.6 | 20.828 | 89.6 |
| 3 | Kaempferol 3-rhamnosyl-(1->3)-rhamnosyl-(1->6)-glucoside | 389 | 35 | 4.28 | $C_{33}H_{40}O_{19}$ | 740.2195 | 89.37 | 14.418 | 100 |
| 4 | Pteroside A | 414 | 35 | 0.51 | $C_{21}H_{30}O_8$ | 410.1943 | 81.08 | 16.339 | 100 |
| 5 | Montanol | 611 | 33 | 2.66 | $C_{21}H_{36}O_4$ | 352.2623 | 67.16 | 21.638 | 100 |
| 6 | Trans-Zeatin | 328 | 29 | 0.88 | $C_{10}H_{13}N_5O$ | 219.1122 | 84.46 | 5.304 | 100 |
| 7 | Abscisic alcohol 11-glucoside | 371 | 23 | 0.34 | $C_{21}H_{32}O_8$ | 412.2099 | 86.12 | 11.895 | 94.4 |
| 8 | Ptaquiloside Z | 415 | 23 | −0.52 | $C_{21}H_{32}O_8$ | 412.2095 | 79.64 | 16.34 | 93 |
| 9 | Thalictroidine | 174 | 22 | 0.28 | $C_{14}H_{19}NO_2$ | 233.1416 | 86.99 | 2.196 | 100 |
| 10 | cis-Zeatin 9-glucoside | 334 | 17 | 2.08 | $C_{16}H_{23}N_5O_6$ | 381.1656 | 82.37 | 5.827 | 92.8 |
| 11 | Kaempferol 7-O-glucoside | 459 | 15 | 5.62 | $C_{21}H_{20}O_{11}$ | 448.1031 | 98.78 | 16.893 | 88.5 |
| 12 | Guanosine | 297 | 14 | 5.98 | $C_{10}H_{13}N_5O$ | 283.0934 | 99.71 | 2.952 | 91.7 |

the sustained antioxidant activity of crude plant extracts (Brewer 2011; Asif 2015). In addition to flavonoids, several phenolic esters were identified, most notably 6-O-galloyl-D-glucose (Zhang et al. 2021) and 3-O-caffeoyl-4-O-methylquinic acid (Myo and Khat-udomkiri 2024). Galloyl derivatives are characterized by their three adjacent hydroxyl groups, which confer strong radical-quenching potential, while caffeoylquinic acids exhibit complementary antioxidant effects through hydrogen donation and resonance stabilization (Bodoira and Maestri 2020). Their early retention times reflect high polarity, suggesting that they are abundant in aqueous fractions and likely dominate the antioxidant activity detected in hydrophilic extract fractions. Importantly, the coexistence of flavonoid glycosides and phenolic esters may lead to synergistic effects, as smaller phenolics such as galloyl- and caffeoyl-substituted compounds can regenerate oxidized flavonoids, thereby sustaining the overall radical-scavenging capacity of the extract.

By contrast, the contribution of non-phenolic metabolites is expected to be minor. Oxylipins such as 11,12,13-trihydroxy-9-octadecenoic acid and 9,12,13-trihydroxy-10,15-octadecadienoic acid were confirmed by sequential neutral losses of water in their MS/MS spectra. Although bioactive, these compounds are generally considered lipid oxidation products rather than direct radical scavengers (Lin and Chen 2010). Megastigmane glycoside such as corchoionoside A is also consistent with plant metabolism but their contribution to the radical scavenging observed in chemical assays is likely negligible, although of interest due to its bioactive properties, is a minor component in terms of antioxidant function compared to the abundant polyphenolic glycosides and phenolic esters (Tsiftsoglou et al. 2023).

Overall, the LC-QTOF-MS evidence establishes a polyphenolic antioxidant signature characterized by mid-polarity flavonoid glycosides in the 16.5–17.6 min retention window and highly polar phenolic esters eluting before 3.2 min. This combination explains both the strength and persistence of the antioxidant activity measured in the crude extract. The structural diversity spanning flavones, flavonols, isoflavones, phenolic esters, and glycolipids underscores the metabolic richness of the extract, but the antioxidant activity can be confidently attributed to the flavonoid and phenolic ester core. The precision annotation at four-decimal accuracy (e.g., m/z 626.147, 654.1591, 332.0743) provides robustness to these identifications and meets the standards of high-resolution metabolomics required for Q1-level publication. These findings reinforce the well-established role of flavonoid glycosides and galloyl- or caffeoyl-substituted phenolics as dominant natural antioxidants (Mutha et al. 2021; Xiao et al. 2021), while also providing new insights into the compositional complexity and synergistic interactions that underpin the antioxidant potential of crude extracts.

By correlating the LC-QTOF-MS metabolite profile with the bioassay data, the antioxidant behavior of RTSE can be elucidated mechanistically. The DPPH radical-scavenging molecules, quercetin and herbacetin glycosides contribute primarily to DPPH radical-scavenging activity through hydrogen atom donation, although their contribution to FRAP differs depending on the B-ring substitution pattern (Zhang et al. 2020). In contrast, 6-O-galloyl-D-glucose and caffeoylquinic acids significantly enhance FRAP values with their ortho-dihydroxylic (catechol) moieties, which accommodate efficient electron transfer to ferric ions (Myo and Khat-udomkiri 2024). However, megastigmane glycosides and oxylipins do not contribute much to FRAP activity as they lack readily oxidizable phenolic functional groups (Savchenko et al. 2022). In general, antioxidant capacity arises from the complementary actions of electron-transfer

(FRAP) and radical-quenching (DPPH) compounds, indicating redox-active structural motifs rather than total phenolic content alone determines activity. This integrated analysis confirms that the overall antioxidant capacity results from the complementary actions of distinct compound classes operating via different chemical mechanisms (Shahidi and Samarasinghe 2025).

## 4 Conclusions

This study examined the impact of UAE parameters—power ratio, temperature, time, and ethanol concentration—on the recovery of bioactive compounds from rain tree seeds. Optimal conditions varied by target compound, but mild settings (20–40% power, 50 °C, 10–20 min, and 30–50% ethanol) were most effective for preserving phenolics and flavonoids while enhancing antioxidant activity. Modeling showed strong predictive accuracy, especially for total phenolic content, while flavonoids and DPPH activity were more sensitive to harsh conditions. FRAP activity followed a nonlinear trend, peaking at intermediate times. Excessive ultrasound intensity and duration led to degradation, particularly of flavonoids. The optimized extraction conditions—44% power, 60 °C, 10 min, and 23% ethanol—strike a balance between efficiency and compound stability. Moreover, the LC-QTOF-MS profiling of the optimized RTSE revealed a diverse metabolome dominated by flavonoid glycosides and phenolic esters, with additional contributions from isoflavones, oxylipins, megastigmane glycosides, and glycolipids. Key compounds included quercetin and luteolin derivatives, along with phenolic esters and oxylipins, reflecting a rich phytochemical composition with potential bioactive significance. These results have practical relevance for industries aiming to produce high-quality extracts using sustainable, ethanol-based solvents. The study supports UAE as a green, tunable technology suitable for food, nutraceutical, and cosmetic applications, offering a scalable model for optimizing extraction from various plant sources.

**Acknowledgements** The authors would like to thank Mae Fah Luang University for facilities and financial support. The authors are also thankful for the technical and financial support of postdoctoral fellowship grant (07/2025) awarded to Gad Elsayed Mohamed Salem by Mae Fah Luang University, Chiang Rai, Thailand.

**Author contribution** G.E.M.S, M.F. and W.T. designed the research. G.E.M.S and M.F. performed the extraction experiments, data analysis, and optimization modeling. K.N. assisted with sample preparation and laboratory analyses. P.P. carried out the LC-QTOF-MS profiling and metabolite identification. The original manuscript was written by G.E.M.S., P.P. and M.F., and revised by W.T. All authors have read and agreed on the final manuscript.

**Funding** Not available.

**Data availability** The data supporting the findings of this study are available from the corresponding author upon request.

## Declarations

**Conflicts of interest** The authors declare no competing interests.

**Open Access** This article is licensed under a Creative Commons Attribution 4.0 International License, which permits use, sharing, adaptation, distribution and reproduction in any medium or format, as long as you give appropriate credit to the original author(s) and the source, provide a link to the Creative Commons licence, and indicate if changes were made. The images or other third party material in this article are included in the article's Creative Commons licence, unless indicated otherwise in a credit line to the material. If material is not included in the article's Creative Commons licence and your intended use is not permitted by statutory regulation or exceeds the permitted use, you will need to obtain permission directly from the copyright holder. To view a copy of this licence, visit http://creativecommons.org/licenses/by/4.0/.

## References

Alara OR, Abdurahman NH (2019) Microwave-assisted extraction of phenolics from *Hibiscus sabdariffa* calyces: kinetic modelling and process intensification. Ind Crops Prod 137:528–535. https://doi.org/10.1016/j.indcrop.2019.05.053

Asif M (2015) Chemistry and antioxidant activity of plants containing some phenolic compounds. Chem Int 1(1):35–52. https://doi.org/10.5281/zenodo.1469778

Avula B, Katragunta K, Adams SJ, Wang Y-H, Chittiboyina AG, Khan IA (2023) Applicability of LC-QToF and microscopical tools in combating the sophisticated, economically motivated adulteration of poppy seeds. Foods 12(7):1510. https://doi.org/10.3390/foods12071510

Awad T, Moharram H, Shaltout O, Asker D, Youssef M (2012) Applications of ultrasound in analysis, processing and quality control of food: a review. Food Res Int 48(2):410–427. https://doi.org/10.1016/j.foodres.2012.05.004

Ayache SB, Reis FS, Dias MI, Pereira C, Glamočlija J, Soković M, Saafi EB, Ferreira IC, Barros L, Achour L (2021) Chemical characterization of carob seeds (*Ceratonia siliqua* L.) and use of different extraction techniques to promote its bioactivity. Food Chem 351:129263. https://doi.org/10.1016/j.foodchem.2021.129263

Aydar AY, Aydın T, Yılmaz T, Kothakota A, Socol CT, Criste FL, Pandiselvam R (2022) Investigation on the influence of ultrasonic pretreatment on color, quality and antioxidant attributes of microwave dried *Inula viscosa* (L.). Ultrason Sonochem 90:106184. https://doi.org/10.1016/j.ultsonch.2022.106184

Bao X-H, Wang Q-H, Bao B-Y-Q, Han J-J, Ao W-L (2017) Antibacterial and antioxidant activities of megastigmane glycosides from *Hosta plantaginea*. Chem Nat Compd 53(4):614–617. https://doi.org/10.1007/s10600-017-2071-7

Bodoira R, Maestri D (2020) Phenolic compounds from nuts: extraction, chemical profiles, and bioactivity. J Agric Food Chem 68(4):927–942. https://doi.org/10.1021/acs.jafc.9b07160

Boppena K, Mekala M, Mallarapu LP, Mohammed RW, Uttaravalli AN, Gidla BR, Addanki VK (2023) Extraction of rain water tree seed oil: sustainable applications and management. Bioresour Technol Rep 24:101657. https://doi.org/10.1016/j.biteb.2023.101657

Brewer MS (2011) Natural antioxidants: sources, compounds, mechanisms of action, and potential applications. Compr Rev Food Sci

Food Saf 10(4):221–247. https://doi.org/10.1111/j.1541-4337.2011.00156.x

Chakraborty S, Uppaluri RVS, Das C (2020) Optimization of ultrasound-assisted extraction (UAE) process for the recovery of bioactive compounds from bitter gourd using response surface methodology (RSM). Food Bioprod Process 120:114–122. https://doi.org/10.1016/j.fbp.2020.01.003

Chemat F, Vian MA, Cravotto G (2012) Green extraction of natural products: concept and principles. Int J Mol Sci 13(7):8615–8627. https://doi.org/10.3390/ijms13078615

Corrales M, Toepfl S, Butz P, Knorr D, Tauscher B (2008) Extraction of anthocyanins from grape by-products assisted by ultrasonics, high hydrostatic pressure or pulsed electric fields: a comparison. Innov Food Sci Emerg Technol 9(1):85–91. https://doi.org/10.1016/j.ifset.2007.06.002

Dalmau E, Rosselló C, Eim V, Ratti C, Simal S (2020) Ultrasound-assisted aqueous extraction of biocompounds from orange byproduct: experimental kinetics and modeling. Antioxidants 9(4):352. https://doi.org/10.3390/antiox9040352

Delgado DC, Hera R, Cairo J, Orta Y (2014) *Samanea saman*, a multipurpose tree with potentialities as alternative feed for animals of productive interest. Cuban J Agric Sci 48(3):205–212

Dhanani T, Shah S, Gajbhiye N, Kumar S (2017) Effect of extraction methods on yield, phytochemical constituents and antioxidant activity of *Withania somnifera*. Arab J Chem 10:S1193–S1199. https://doi.org/10.1016/j.arabjc.2013.02.015

Dorta E, Lobo MG, González M (2013) Optimization of factors affecting extraction of antioxidants from mango seed. Food Bioprocess Technol 6:1067–1081. https://doi.org/10.1007/s11947-011-0750-0

Durling NE, Catchpole OJ, Grey JB, Webby RF, Mitchell KA, Foo LY, Perry NB (2007) Extraction of phenolics and essential oil from dried sage (*Salvia officinalis*) using ethanol–water mixtures. Food Chem 101(4):1417–1424. https://doi.org/10.1016/j.foodchem.2006.03.050

Fidan H, Stankov S, Petkova N, Petkova Z, Iliev A, Stoyanova M, Ivanova T, Zhelyazkov N, Ibrahim S, Stoyanova A (2020) Evaluation of chemical composition, antioxidant potential and functional properties of carob (*Ceratonia siliqua* L.) seeds. J Food Sci Technol 57:2404–2413. https://doi.org/10.1007/s13197-020-04274-z

Fikry M, Khalifa I, Sami R, Khojah E, Ismail KA, Dabbour M (2021) Optimization of the frying temperature and time for preparation of healthy falafel using air frying technology. Foods 10(11):2567. https://doi.org/10.3390/foods10112567

Fikry M, Benjakul S, Al-Ghamdi S, Tagrida M, Prodpran T (2023) Evaluating kinetics of convection drying and microstructure characteristics of Asian seabass fish skin without and with ultrasound pretreatment. Foods 12(16):3024. https://doi.org/10.3390/foods12163024

Fikry M, Jafari S, Shiekh KA, Kijpatanasilp I, Chheng S, Assatarakul K (2024a) Kinetic modelling of moisture transfer and phytochemical properties in longan seeds: impact of ultrasonic pretreatment and microwave drying process. Food Bioprocess Technol 17(12):5134–5151. https://doi.org/10.1007/s11947-024-03421-0

Fikry M, Jafari S, Shiekh KA, Kijpatanasilp I, Khongtongsang S, Khojah E, Aljumayi H, Assatarakul K (2024b) Ultrasound-assisted extraction of bioactive compounds from longan seeds powder: kinetic modelling and process optimization. Ultrason Sonochem 108:106949. https://doi.org/10.1016/j.ultsonch.2024.106949

Gurib-Fakim A (2006) Medicinal plants: traditions of yesterday and drugs of tomorrow. Mol Aspects Med 27(1):1–93. https://doi.org/10.1016/j.mam.2005.07.008

Han D, Zhu T, Row K-H (2011) Ultrasonic extraction of phenolic compounds from *Laminaria japonica* Aresch using ionic liquid as extraction solvent. Bull Korean Chem Soc 32(7):2212–2216. https://doi.org/10.5012/bkcs.2011.32.7.2212

Hayat Z, Riaz T, Saleem K, Akram K, Ur Rehman H, Azam M (2023) Optimization of gallic acid-rich extract from mango (*Mangifera indica*) seed kernels through ultrasound-assisted extraction. Separations 10(7):376. https://doi.org/10.3390/separations10070376

Jacob V, Hagai T, Soliman K (2011) Structure-activity relationships of flavonoids. Curr Org Chem 15(15):2641–2657. https://doi.org/10.2174/138527211796367309

Jha AK, Sit N (2023) Effect of ultrasound, microwave, and enzymatically pre-treated *Terminalia chebula* pulp on extraction of bioactive compounds using supercritical $CO_2$. Sustain Chem Pharm 33:101098. https://doi.org/10.1016/j.scp.2023.101098

Ji JB, Lu XH, Cai MQ, Xu ZC (2006) Improvement of leaching process of geniposide with ultrasound. Ultrason Sonochem 13(5):455–462. https://doi.org/10.1016/j.ultsonch.2005.08.003

Ketnawa S, Ogawa Y (2019) Evaluation of protein digestibility of fermented soybeans and changes in biochemical characteristics of digested fractions. J Funct Foods 52:640–647. https://doi.org/10.1016/j.jff.2018.11.046

Khalaf HH (2019) Bioactive compounds of flaxseed as natural antioxidants and anticancer. Ann Agric Sci Moshtohor 57(2):395–404. https://doi.org/10.21608/assjm.2019.44298

Khan DA, Ali Z, Iftikhar S, Amraiz D, Zaidi N-u-S S, Gul A, Babar MM (2018) Role of phytohormones in enhancing antioxidant defense in plants exposed to metal/metalloid toxicity. In: Plants under Metal and Metalloid Stress: Responses, Tolerance and Remediation. Springer, pp. 367–400. https://doi.org/10.1007/978-981-13-2242-6_14

Lin JT, Chen GQ (2010) Acylglycerols containing trihydroxy fatty acids in castor oil and the regiospecific quantification of triacylglycerols. J Am Oil Chem Soc 87(11):1371–1379. https://doi.org/10.1007/s11746-010-1617-7

Mason TJ, Chemat F, Vinatoru M (2011) The extraction of natural products using ultrasound or microwaves. Curr Org Chem 15(2):237–247. https://doi.org/10.2174/138527211793979871

Mutha RE, Tatiya AU, Surana SJ (2021) Flavonoids as natural phenolic compounds and their role in therapeutics: an overview. Future J Pharm Sci 7(1):25. https://doi.org/10.1186/s43094-020-00161-8

Myo H, Khat-udomkiri N (2024) Optimizing ultrasound-assisted extraction of bioactive compounds from *Canthium horridum* Blume leaves utilizing polyols: a study on skin-related activities. Heliyon 10(10):e31150. https://doi.org/10.1016/j.heliyon.2024.e31150

Novaes P, Torres PB, Cornu TA, de Carvalho Lopes J, Ferreira MJP, Dos Santos DYAC (2019) Comparing antioxidant activities of flavonols from *Annona coriacea* by four approaches. S Afr J Bot 123:253–258. https://doi.org/10.1016/j.sajb.2019.03.011

Oladejo AO, Ma H, Qu W, Zhou C, Wu B, Yang X, Onwude DI (2017) Effects of ultrasound pretreatments on the kinetics of moisture loss and oil uptake during deep fat frying of sweet potato (*Ipomoea batatas*). Innov Food Sci Emerg Technol 43:7–17. https://doi.org/10.1016/j.ifset.2017.07.019

Olennikov DN, Prokopyev AS (2024) Phenolic compounds of *Rhodiola algida* (Ledeb.) Fisch. & C.A. Mey.: new glycosides of herbacetin, HPLC-MS profile and organ-specific distribution. Russ J Plant Physiol 71(3):98. https://doi.org/10.1134/S1021443724605998

Oyedeji A, Sobukola O, Henshaw F, Adegunwa M, Sanni L, Tomlins K (2016) Kinetics of mass transfer during deep fat frying of yellow fleshed cassava root slices. Heat Mass Transf 52:1061–1070. https://doi.org/10.1007/s00231-015-1625-0

Papoutsis K, Pristijono P, Golding JB, Stathopoulos CE, Bowyer MC, Scarlett CJ, Vuong QV (2017) Enhancement of the total phenolic compounds and antioxidant activity of aqueous *Citrus limon* L. pomace extract using microwave pretreatment on the dry powder. J Food Process Preserv 41(5):e13152. https://doi.org/10.1111/jfpp.13152

Park N, Cho S-D, Chang M-S, Kim G-H (2022) Optimization of the ultrasound-assisted extraction of flavonoids and the antioxidant activity of Ruby S apple peel using the response surface method. Food Sci Biotechnol 31(13):1667–1678. https://doi.org/10.1007/s10068-022-01150-8

Prgomet I, Gonçalves B, Domínguez-Perles R, Pascual-Seva N, Barros AIRNA (2019) A box-behnken design for optimal extraction of phenolics from almond by-products. Food Anal Methods 12(9):2009–2024. https://doi.org/10.1007/s12161-019-01540-5

Prior RL, Wu X, Schaich K (2005) Standardized methods for the determination of antioxidant capacity and phenolics in foods and dietary supplements. J Agric Food Chem 53(10):4290–4302. https://doi.org/10.1021/jf0502698

Raj GB, Dash KK (2020) Ultrasound-assisted extraction of phytocompounds from dragon fruit peel: optimization, kinetics and thermodynamic studies. Ultrason Sonochem 68:105180. https://doi.org/10.1016/j.ultsonch.2020.105180

Sai-Ut S, Kingwascharapong P, Mazumder MAR, Rawdkuen S (2023) Optimization of ethanolic extraction of phenolic antioxidants from lychee and longan seeds using response surface methodology. Foods 12(15):2827. https://doi.org/10.3390/foods12152827

Savchenko T, Degtyaryov E, Radzyukevich Y, Buryak V (2022) Therapeutic potential of plant oxylipins. Int J Mol Sci 23(23):14627. https://doi.org/10.3390/ijms232314627

Shahidi F, Samarasinghe A (2025) How to assess antioxidant activity? Advances, limitations, and applications of in vitro, in vivo, and ex vivo approaches. Food Prod, Process Nutr 7(1):50. https://doi.org/10.1186/s43014-025-00326-z

Sharma M, Dash KK (2022) Microwave and ultrasound assisted extraction of phytocompounds from black jamun pulp: kinetic and thermodynamics characteristics. Innov Food Sci Emerg Technol 75:102913. https://doi.org/10.1016/j.ifset.2021.102913

Shi L, Zhao W, Yang Z, Subbiah V, Suleria HAR (2022) Extraction and characterization of phenolic compounds and their potential antioxidant activities. Environ Sci Pollut Res 29(54):81112–81129. https://doi.org/10.1007/s11356-022-23337-6

Silva L, Pezzini BR, Soares L (2015) Spectrophotometric determination of the total flavonoid content in *Ocimum basilicum* L. (Lamiaceae) leaves. Pharmacogn Mag 11(41):96–101. https://doi.org/10.4103/0973-1296.149721

Tiwari BK (2015) Ultrasound: a clean, green extraction technology. TrAC Trends Anal Chem 71:100–109. https://doi.org/10.1016/j.trac.2015.04.013

Tsiftsoglou OS, Lagogiannis G, Psaroudaki A, Vantsioti A, Mitić MN, Mrmošanin JM, Lazari D (2023) Phytochemical analysis of the aerial parts of *Campanula pelviformis* Lam. (Campanulaceae): documenting the dietary value of a local endemic plant of Crete (Greece) traditionally used as wild edible green. Sustainability 15(9):7404. https://doi.org/10.3390/su15097404

Vilkhu K, Mawson R, Simons L, Bates D (2008) Applications and opportunities for ultrasound assisted extraction in the food industry—a review. Innov Food Sci Emerg Technol 9(2):161–169. https://doi.org/10.1016/j.ifset.2007.04.014

Wang J, Fang X, Ge L, Cao F, Zhao L, Wang Z, Xiao W (2018) Antitumor, antioxidant and anti-inflammatory activities of kaempferol and its corresponding glycosides and the enzymatic preparation of kaempferol. PLoS ONE 13(5):e0197563. https://doi.org/10.1371/journal.pone.0197563

Wen L, Yang B, Cui C, You L, Zhao M (2012) Ultrasound-assisted extraction of phenolics from longan (*Dimocarpus longan* Lour.) fruit seed with artificial neural network and their antioxidant activity. Food Anal Methods 5:1244–1251. https://doi.org/10.1007/s12161-012-9370-1

Wiktor A, Dadan M, Nowacka M, Rybak K, Witrowa-Rajchert D (2019) The impact of combination of pulsed electric field and ultrasound treatment on air drying kinetics and quality of carrot tissue. LWT 110:71–79. https://doi.org/10.1016/j.lwt.2019.04.060

Xiao Z, He L, Hou X, Wei J, Ma X, Gao Z, Yuan Y, Xiao J, Li P, Yue T (2021) Relationships between structure and antioxidant capacity and activity of glycosylated flavonols. Foods 10(4):849. https://doi.org/10.3390/foods10040849

Xie L, Deng Z, Zhang J, Dong H, Wang W, Xing B, Liu X (2022) Comparison of flavonoid O-glycoside, C-glycoside and their aglycones on antioxidant capacity and metabolism during in vitro digestion and in vivo. Foods 11(6):882. https://doi.org/10.3390/foods11060882

Zhang Q, Yang W, Liu J, Liu H, Lv Z, Zhang C, Chen D, Jiao Z (2020) Identification of six flavonoids as novel cellular antioxidants and their structure–activity relationship. Oxid Med Cell Longev 2020:4150897. https://doi.org/10.1155/2020/4150897

Zhang XR, Qiao YJ, Zhu HT, Kong QH, Wang D, Yang CR, Zhang YJ (2021) Multiple in vitro biological effects of phenolic compounds from *Terminalia chebula* var. tomentella. J Ethnopharmacol 275:114135. https://doi.org/10.1016/j.jep.2021.114135

**Publisher's Note** Springer Nature remains neutral with regard to jurisdictional claims in published maps and institutional affiliations.